Supplement of The SPARC water vapor sssessment II: assessment of satellite measurements of upper tropospheric water vapor

William Read[1], Gabriele Stiller[2], Stefan Lossow[2], Michael Kiefer[2], Farahnaz Khosrawi[2], Dale Hurst[3], Holger Vömel[4], Karen Rosenlof[5], Bianca M. Dinelli[6], Piera Raspollini[7], Gerald E. Nedoluha[8], John C. Gille[9,10], Yasuko Kasai[11], Patrick Eriksson[12], Christopher E. Sioris[13], Kaley A. Walker[14], Katja Weigel[15], John P. Burrows[15], and Alexei Rozanov[15]

[1]Jet Propulsion Laboratory, California Institute of Technology, Pasadena, Ca., USA.
[2]Karlsruhe Institute of Technology, Institute of Meteorology and Climate Research, Karlsruhe, Germany.
[3]Global Monitoring Division, NOAA, Earth System Research Laboratory, Boulder, Colorado, USA.
[4]Earth Observing Laboratory, National Center for Atmospheric Research, Boulder, Colorado, USA.
[5]Chemical Science Division, NOAA, Earth System Research Laboratory, Boulder, Colorado, USA.
[6]Instituto di Scienze dell'Atmosfera e del Clima del Consiglio Nazionale delle Ricerche (ISAC-CNR), Via Gobetti, 101, 40129 Bologna, Italy.
[7]Instituto di Fisica Applicata del Consiglio Nazionale delle Ricerche (IFAC-CNR), Via Madonna del Piano, 10, 50019 Sesto Fiorentino, Italy.
[8]Naval Research Laboratory, Remote Sensing Division, 4555 Overlook Avenue Southwest, Washington, DC 20375, USA.
[9]National Center for Atmospheric Research, Atmospheric Chemistry Observations & Modeling Laboratory, P.O. Box 3000, Boulder, CO. 80307-3000, USA.
[10]University of Colorado, Atmospheric and Oceanic Sciences, Boulder, CO 80309-0311, USA.
[11]National Institute of Information and Communications Technology (NICT), 20 THz Research Center, 4-2-1 Nukui-kita, Koganei, Tokyo 184–8795, Japan.
[12]Chalmers University of Technology, Department of Space, Earth and Environment, Hörsalsvägen 11, 41296 Göteborg, Sweden.
[13]York University, Center for Research in Earth and Space Science, 4700 Keele Street, Toronto, Ontario M3J 1P3, Canada.
[14]University of Toronto, Department of Physics, 60 St. George Street, Toronto, Ontario M5S 1A7, Canada.
[15]University of Bremen, Institute of Environmental Physics, Otto-Hahn-Allee 1, 28334 Breman, Germany.

Correspondence: Read (william.g.read@jpl.nasa.gov)

S1 Introduction

Figures S1–S30 show coincident scatter plots for several instruments versus MLS-Aura or MIPAS-ESA either as a probability density function (PDF, Figure 16 in the main manuscript) or as a scatter of the individual coincidences when their number are few. Figures S31–S33 Show gridded mapped comparisons for other heights in the same format as Figure 21 in the main manuscript. Figures S34–S36 Show a scatter plot of the grid box averages for other heights in the same format as Figure 22 in the main manuscript. Figures S37–S39 Show mapped humidity fields for the SMILES products for several heights in the

same format as Figure 21 in the main manuscript. Figures S40–S42 Show a scatter plot of the grid box averages for SMILES humidity product versus MLS-Aura for several heights in the same format as Figure 22 in the main manuscript. Figures S43–S44 Show mapped humidity fields for the occultation instruments for several heights in the same format as Figure 21 in the main manuscript. Figures S45–S46 Show a scatter plot of the grid box averages for the occultation instruments versus MLS-Aura for several heights in the same format as Figure 22 in the main manuscript.

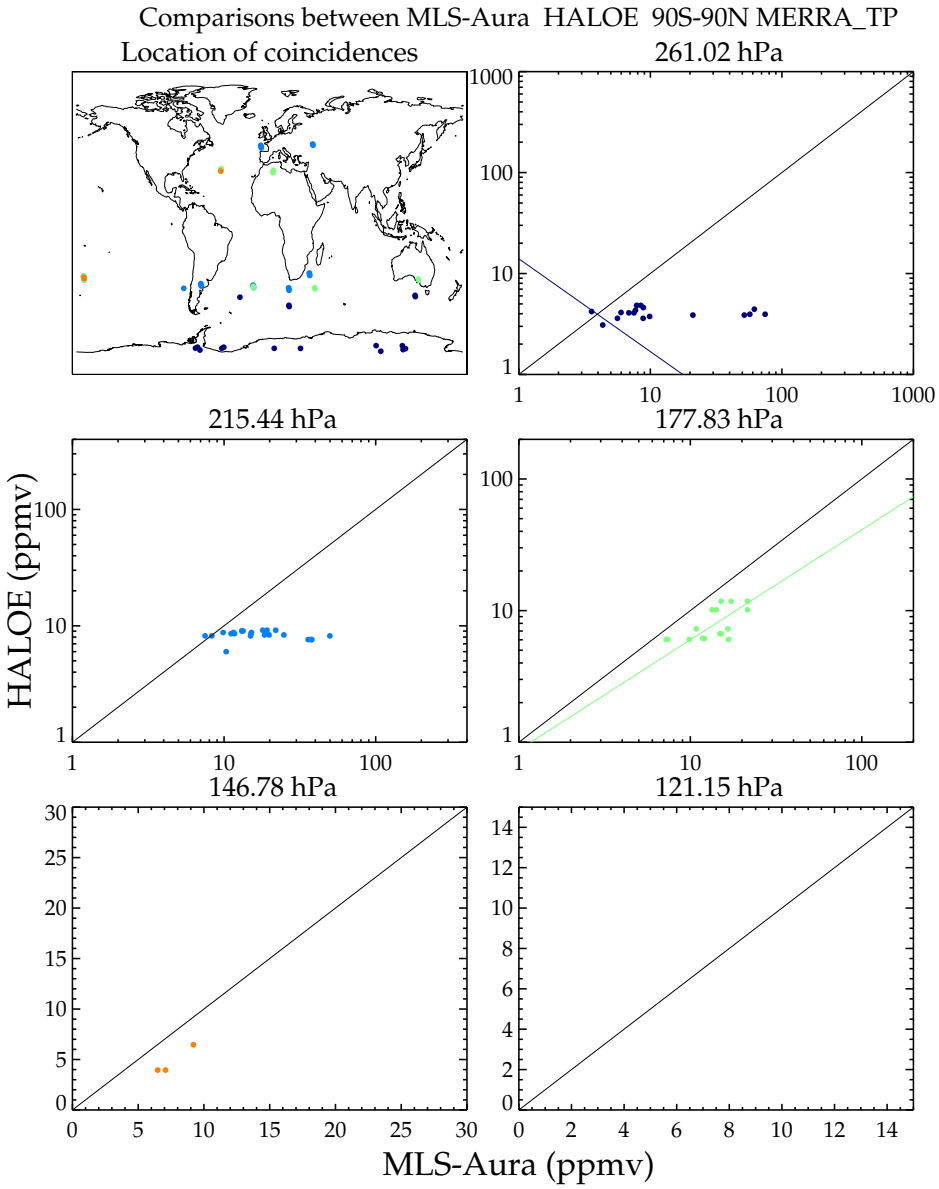

Figure S1. Scatter plot of coincident humidity measurements between MLS-Aura and HALOE

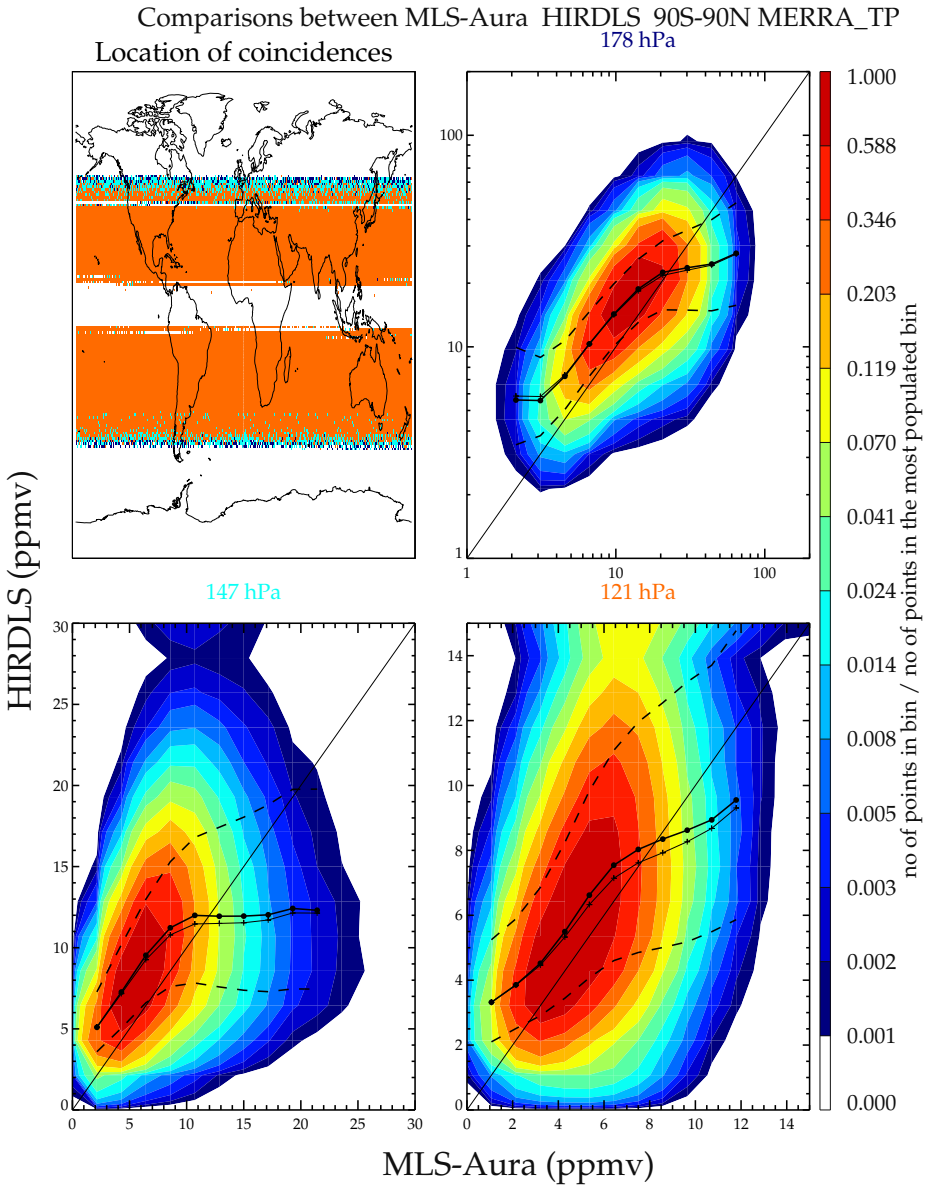

Figure S2. Scatter plot of coincident humidity measurements between MLS-Aura and HIRDLS

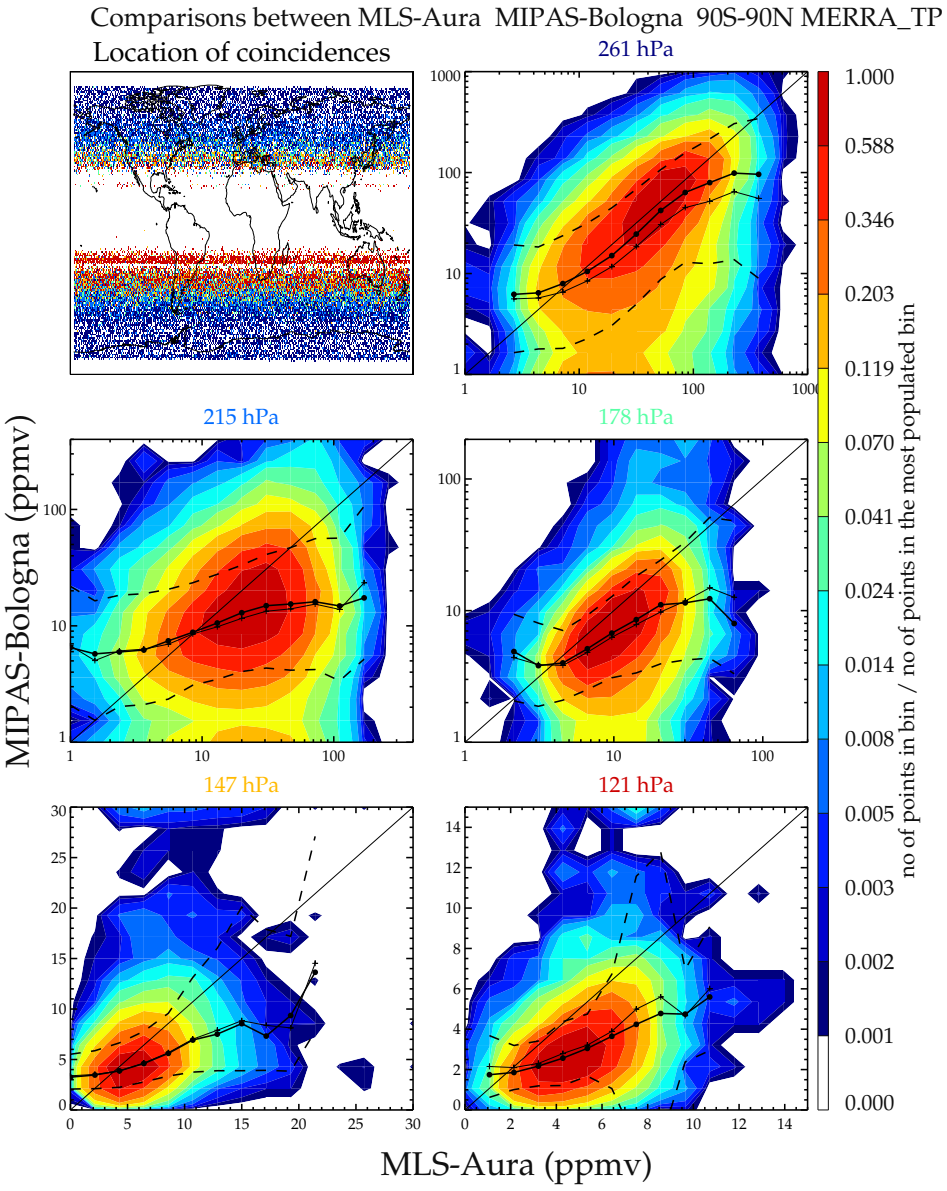

Figure S3. Scatter plot of coincident humidity measurements between MLS-Aura and MIPAS-Bologna

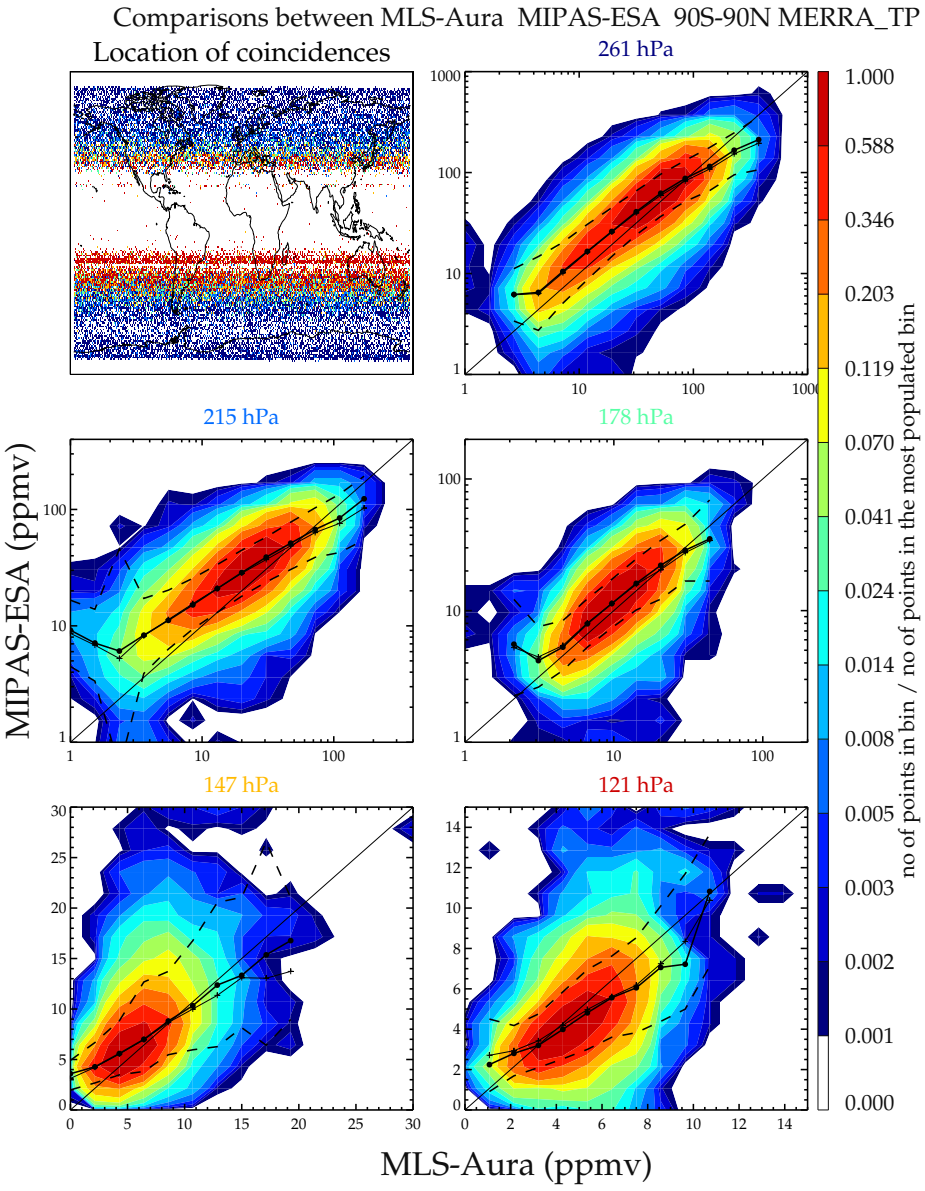

Figure S4. Scatter plot of coincident humidity measurements between MLS-Aura and MIPAS-ESA

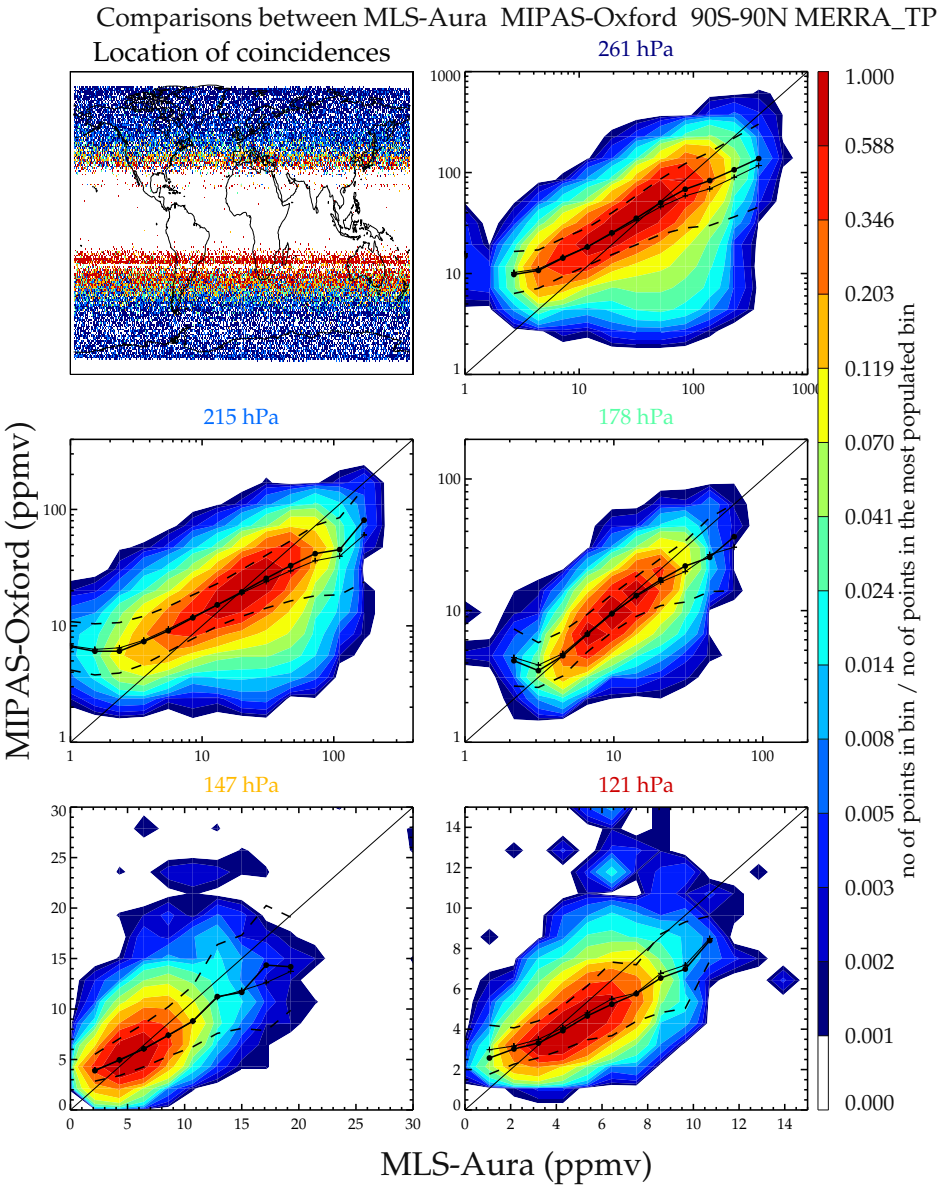

Figure S5. Scatter plot of coincident humidity measurements between MLS-Aura and MIPAS-Oxford

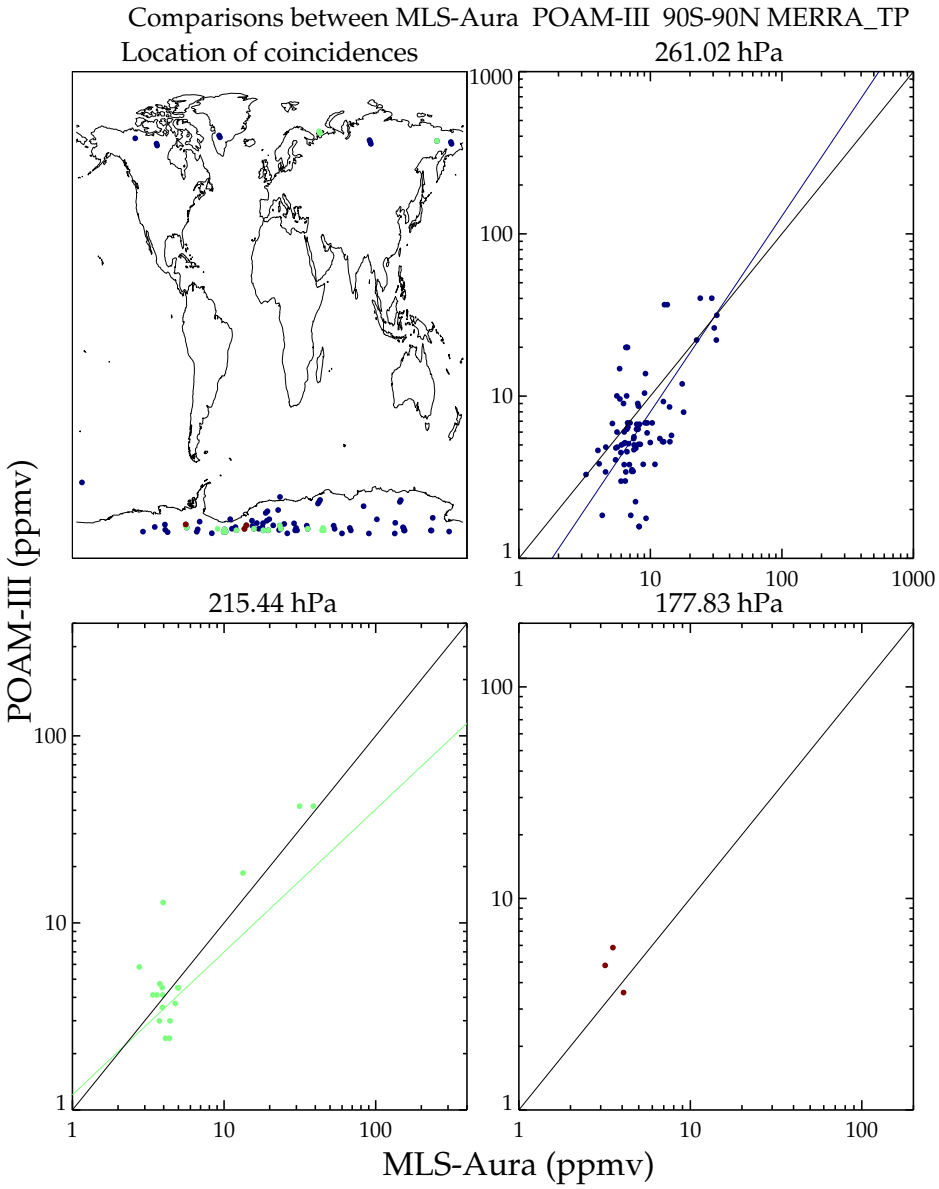

Figure S6. Scatter plot of coincident humidity measurements between MLS-Aura and POAM-III

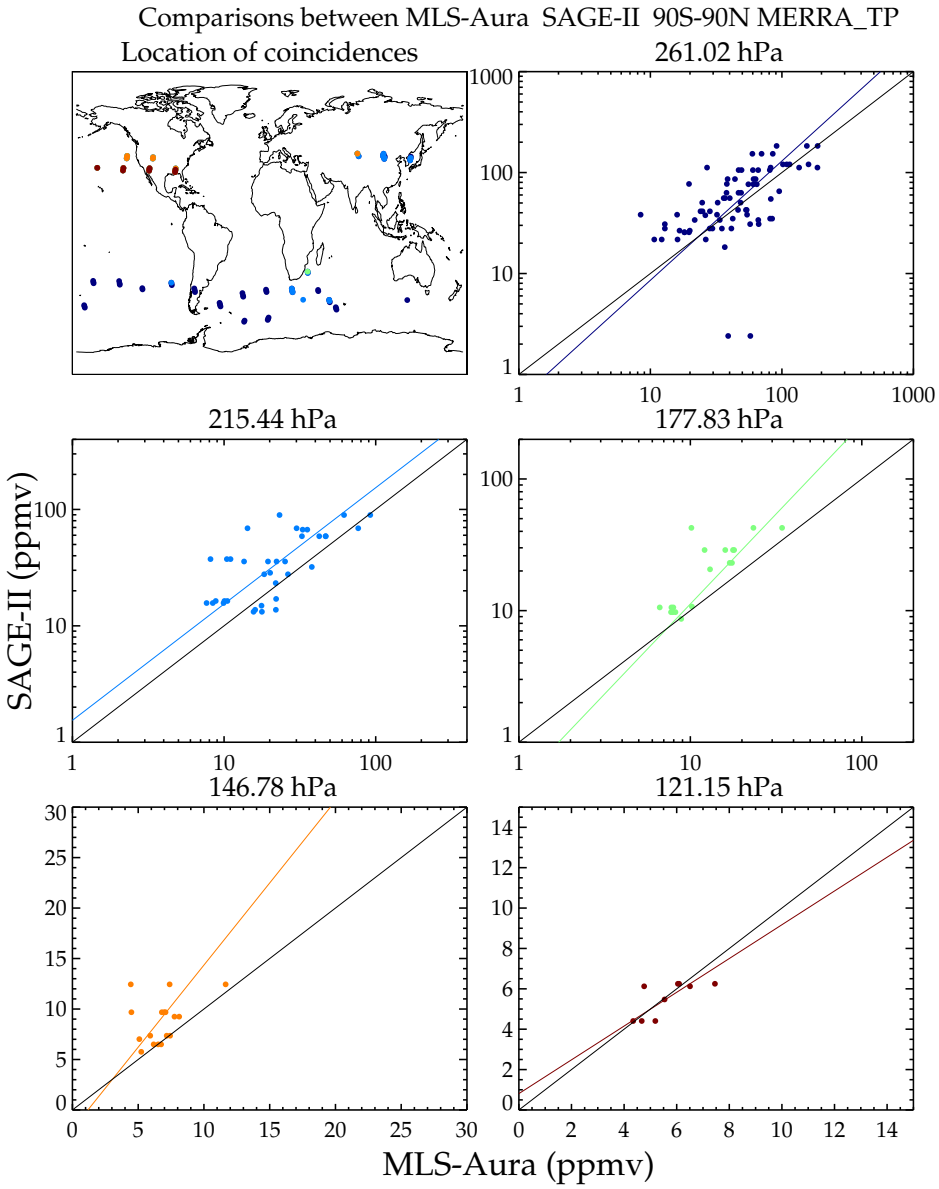

Figure S7. Scatter plot of coincident humidity measurements between MLS-Aura and SAGE-II

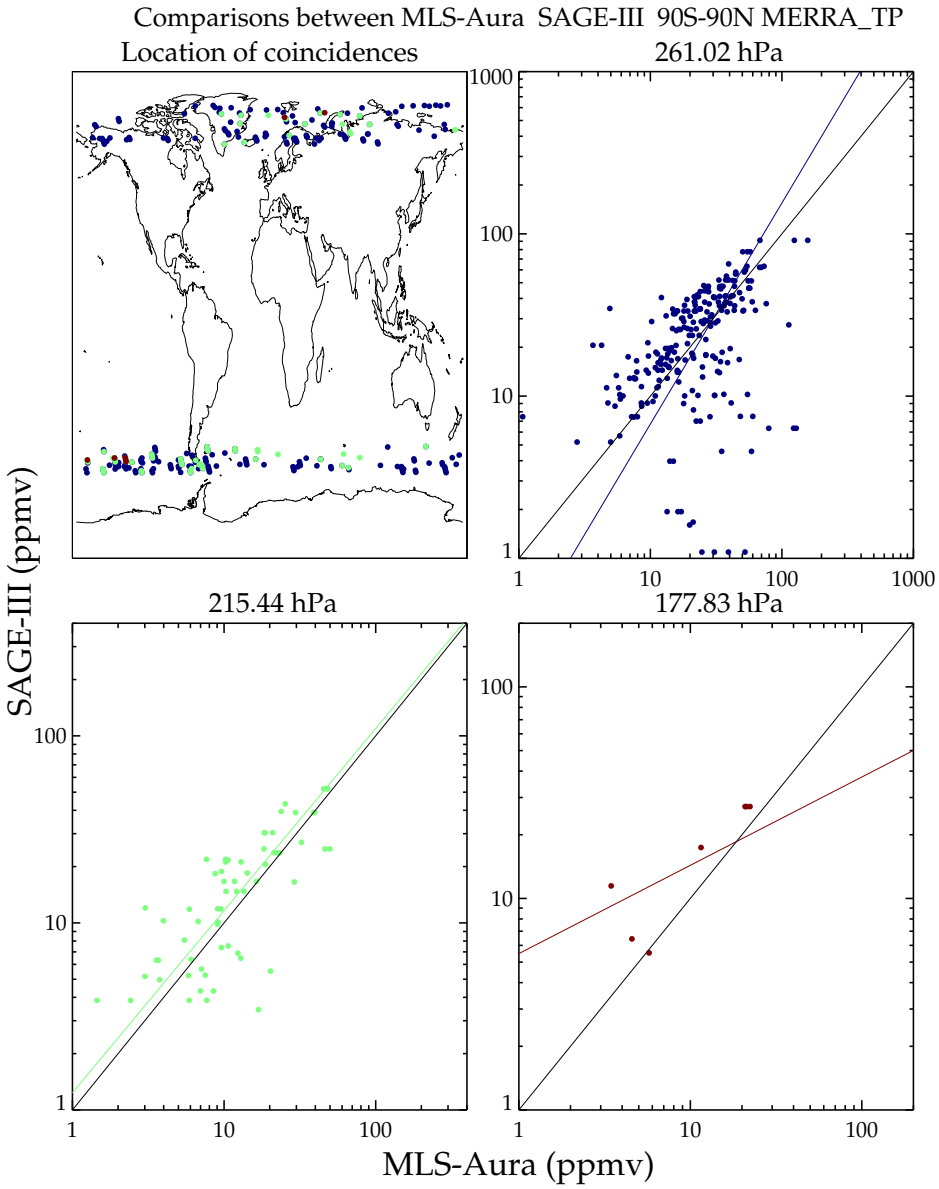

Figure S8. Scatter plot of coincident humidity measurements between MLS-Aura and SAGE-III

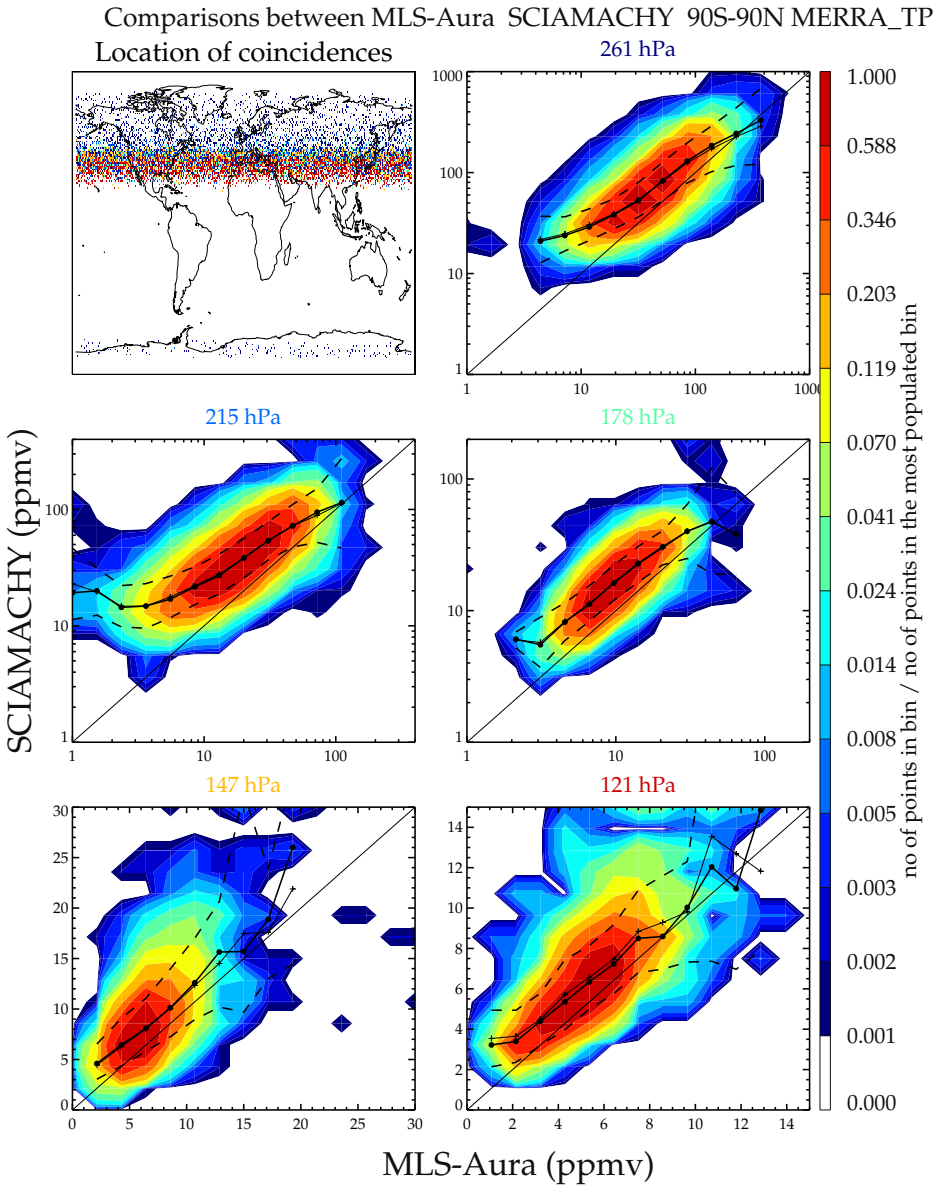

Figure S9. Scatter plot of coincident humidity measurements between MLS-Aura and SCIAMACHY

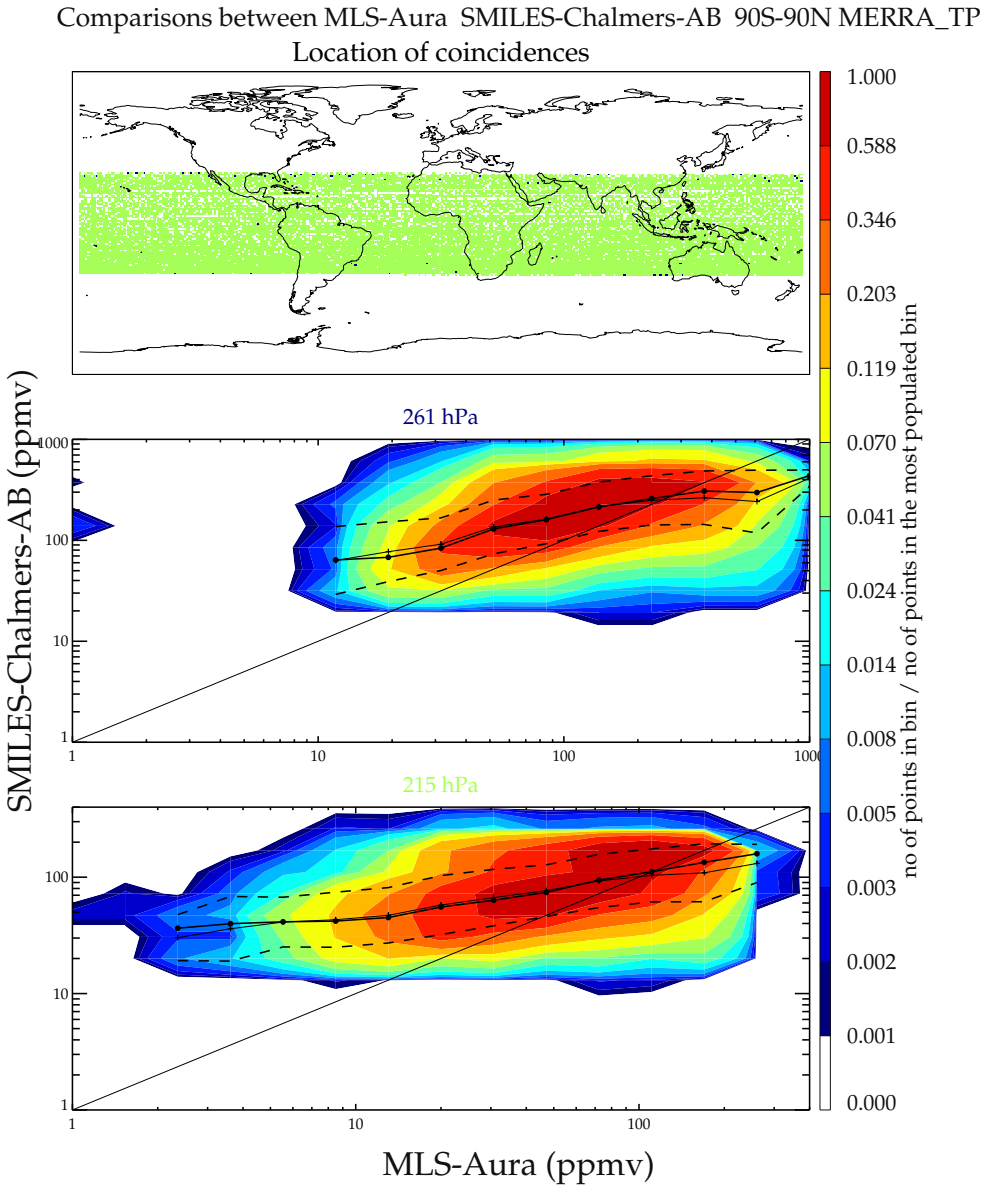

Figure S10. Scatter plot of coincident humidity measurements between MLS-Aura and SMILES Chalmers AB

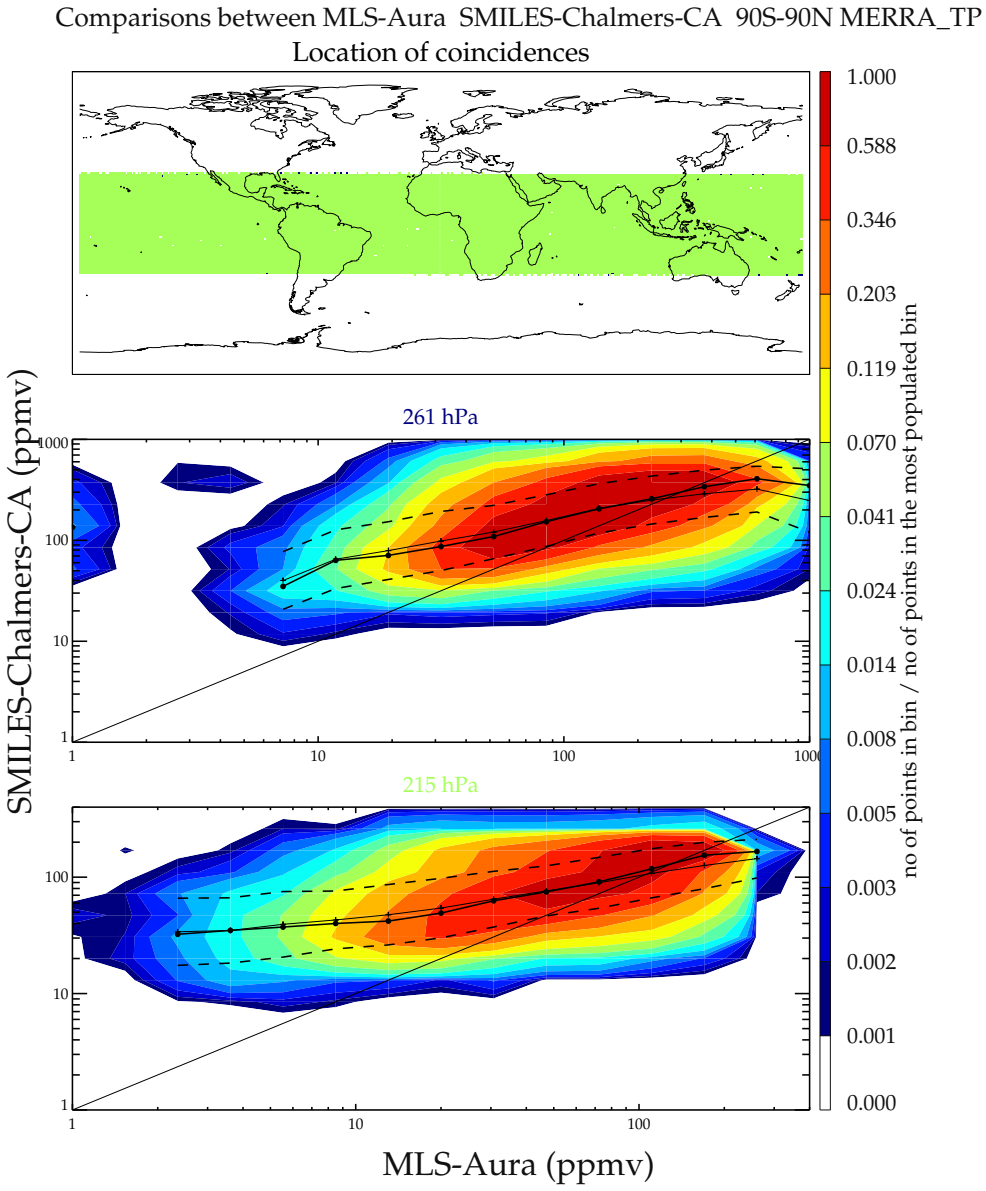

Figure S11. Scatter plot of coincident humidity measurements between MLS-Aura and SMILES Chalmers CA

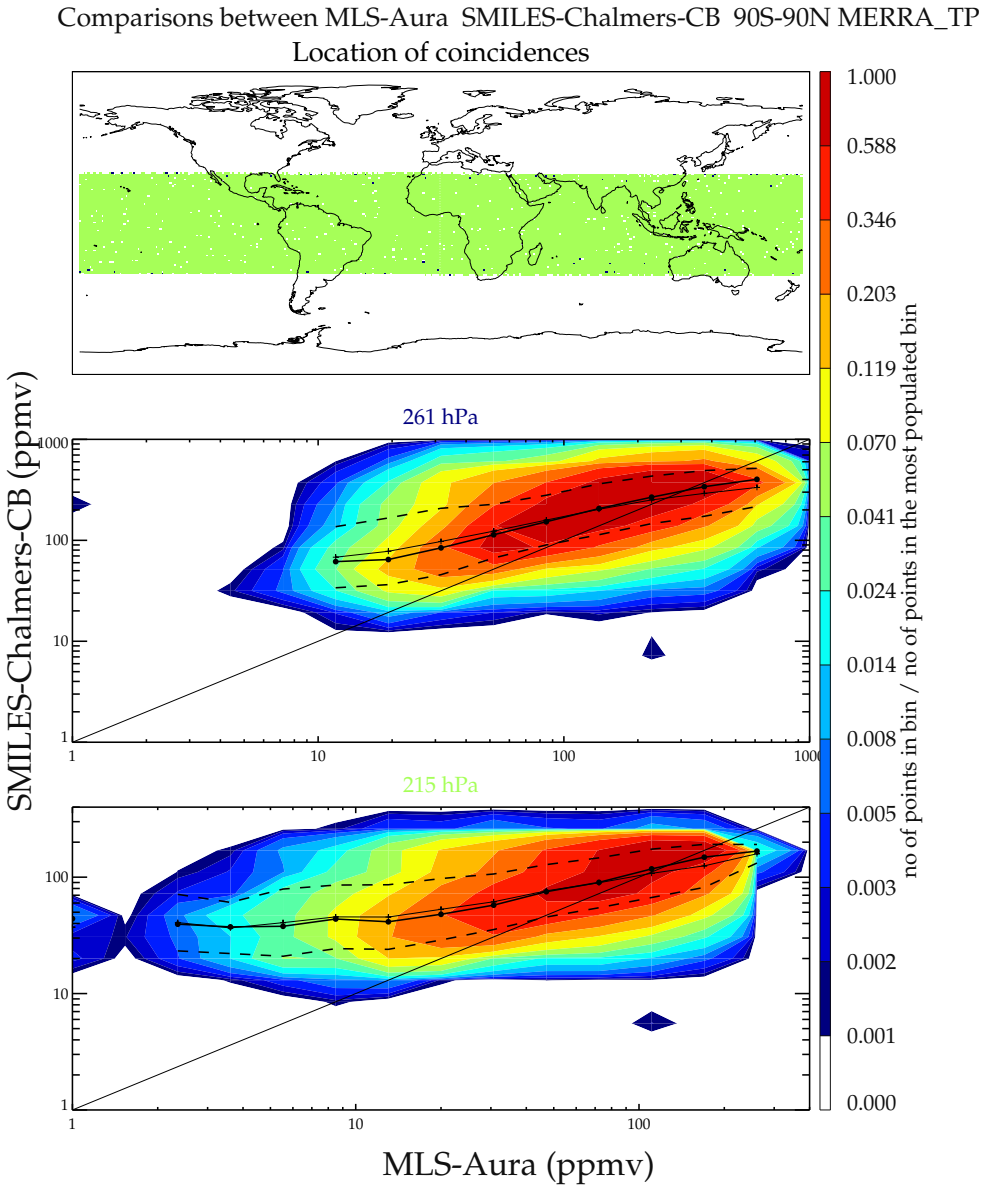

Figure S12. Scatter plot of coincident humidity measurements between MLS-Aura and SMILES Chalmers CB

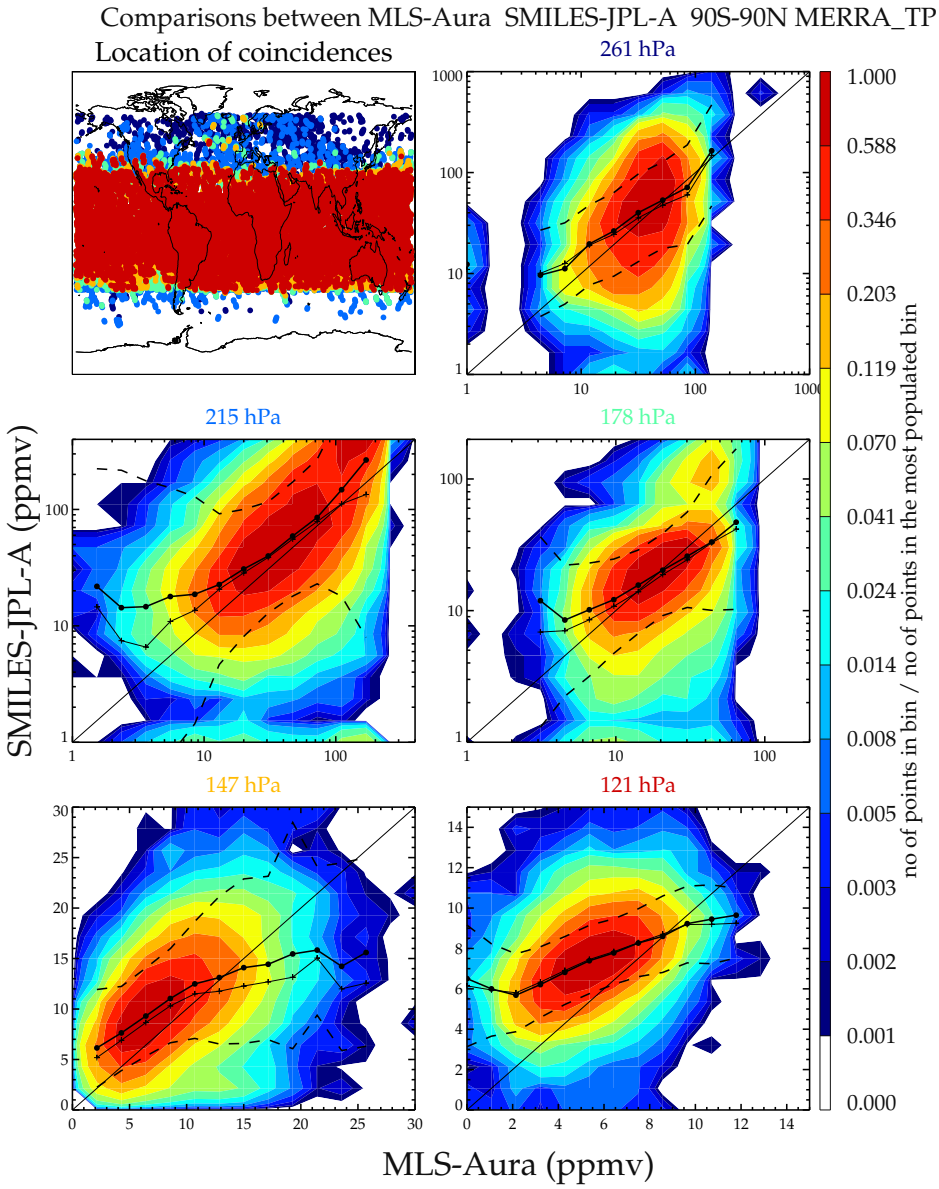

Figure S13. Scatter plot of coincident humidity measurements between MLS-Aura and SMILES JPL A

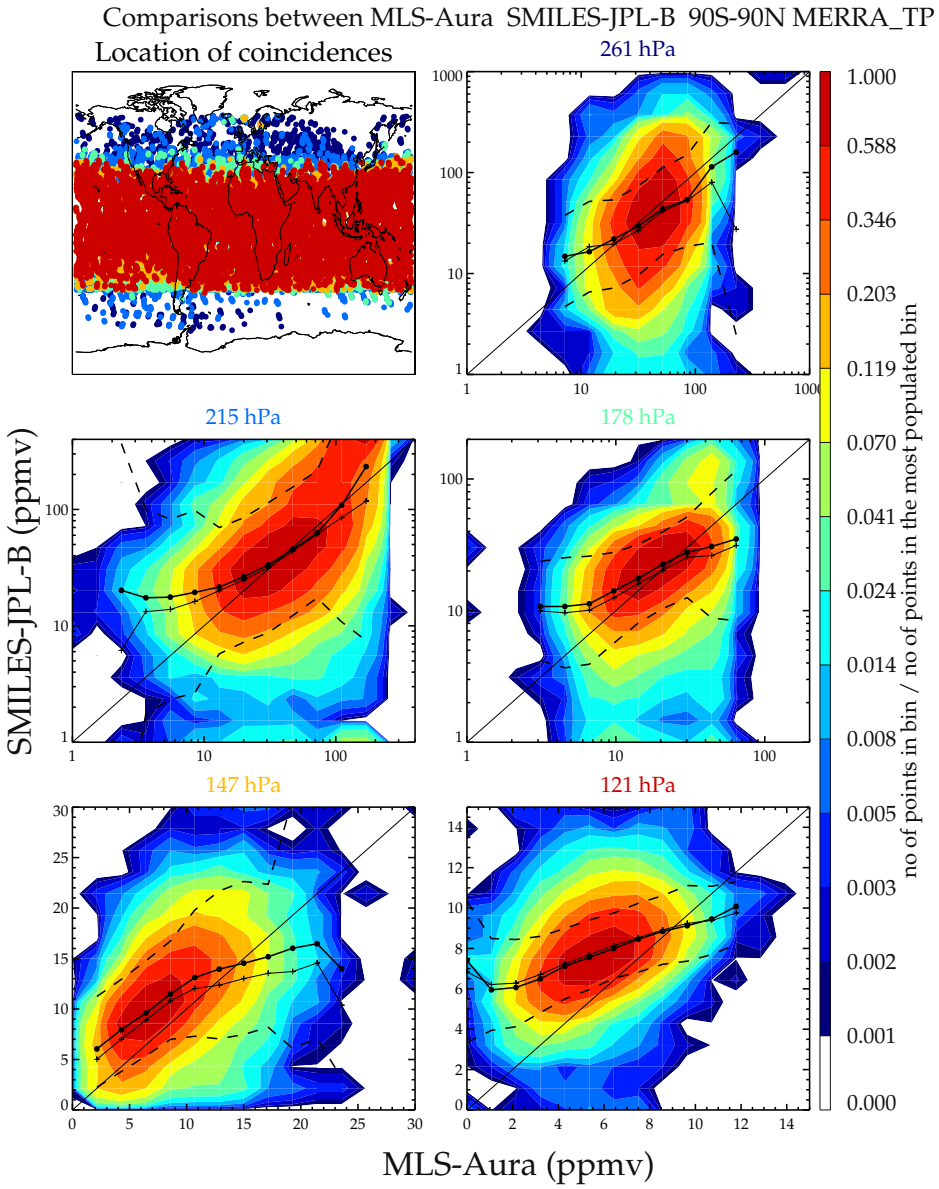

Figure S14. Scatter plot of coincident humidity measurements between MLS-Aura and SMILES JPL B

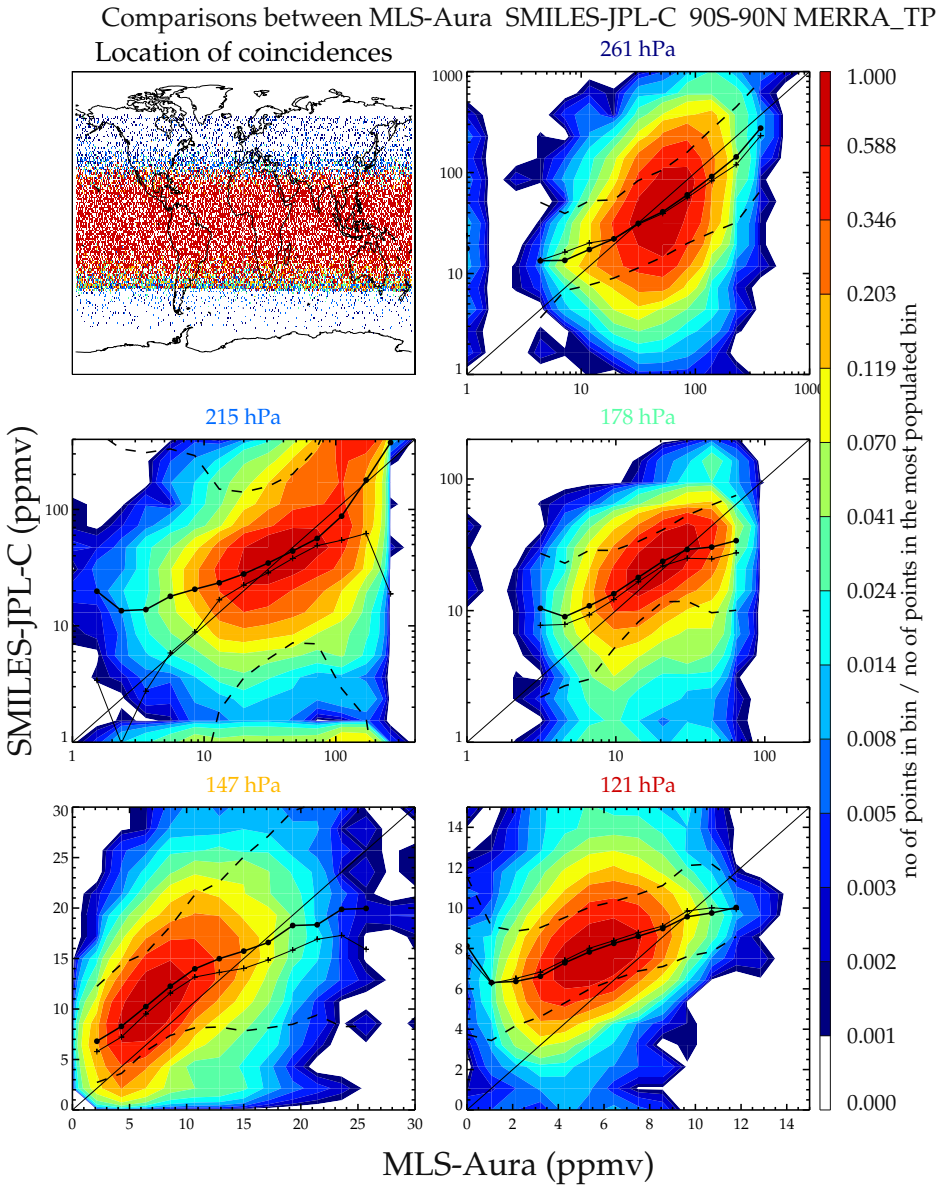

Figure S15. Scatter plot of coincident humidity measurements between MLS-Aura and SMILES JPL C

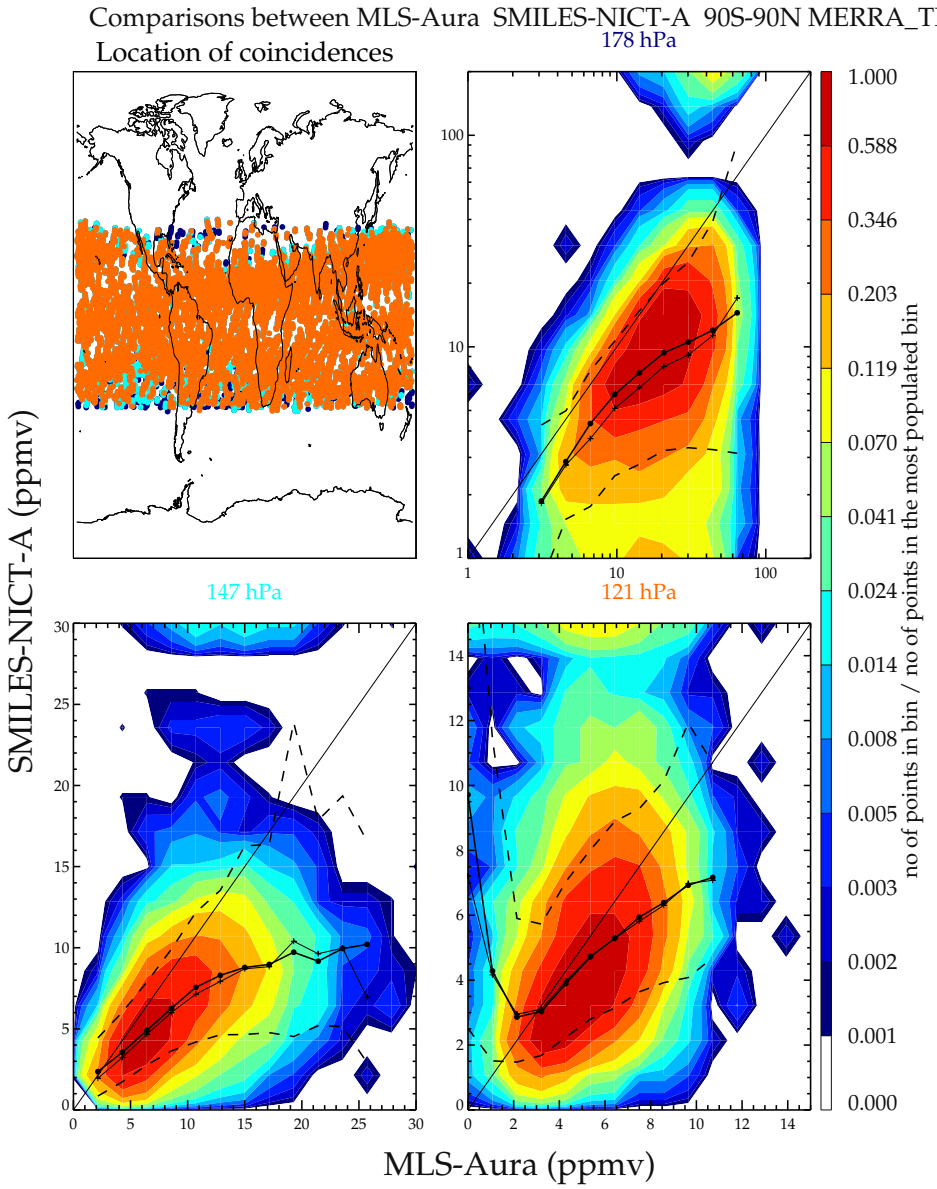

Figure S16. Scatter plot of coincident humidity measurements between MLS-Aura and SMILES NICT A

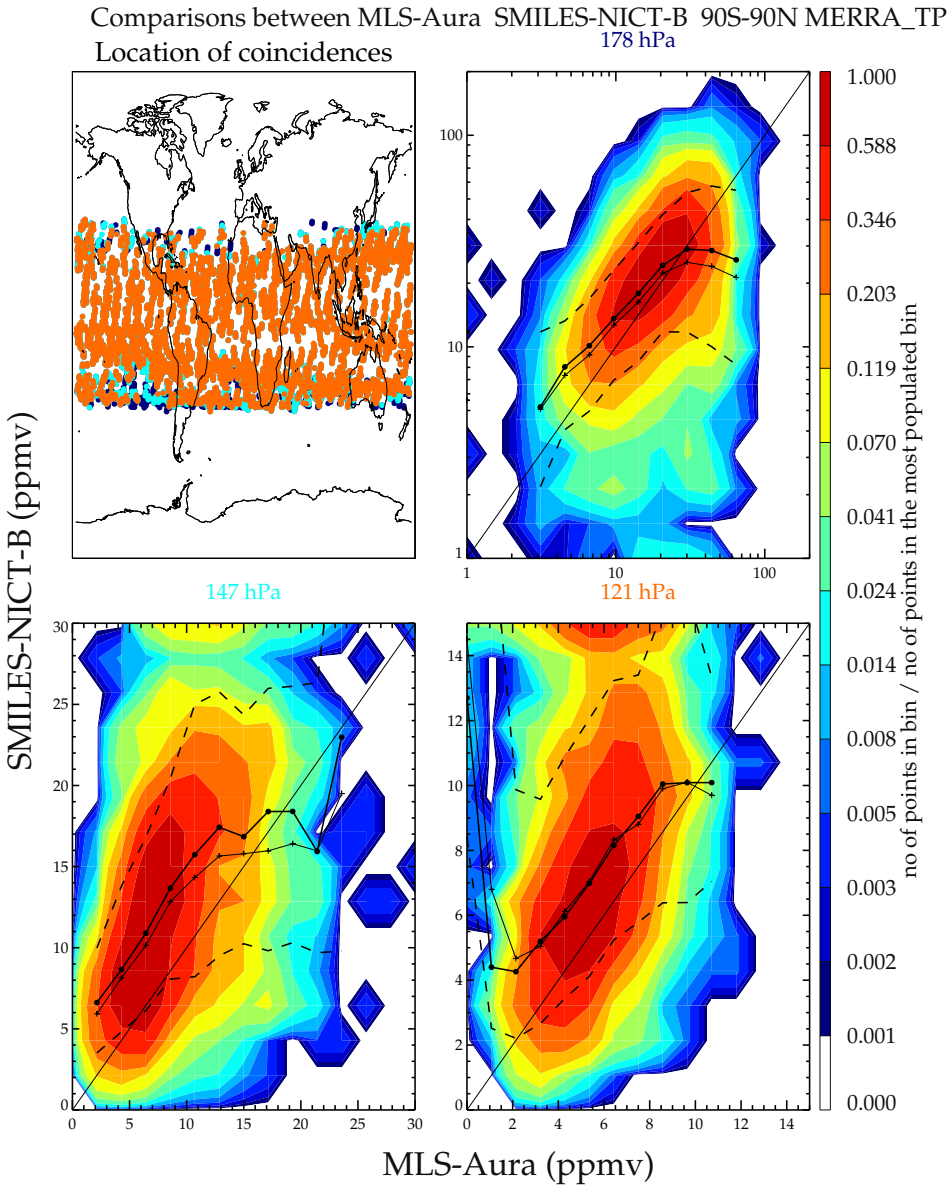

Figure S17. Scatter plot of coincident humidity measurements between MLS-Aura and SMILES NICT B

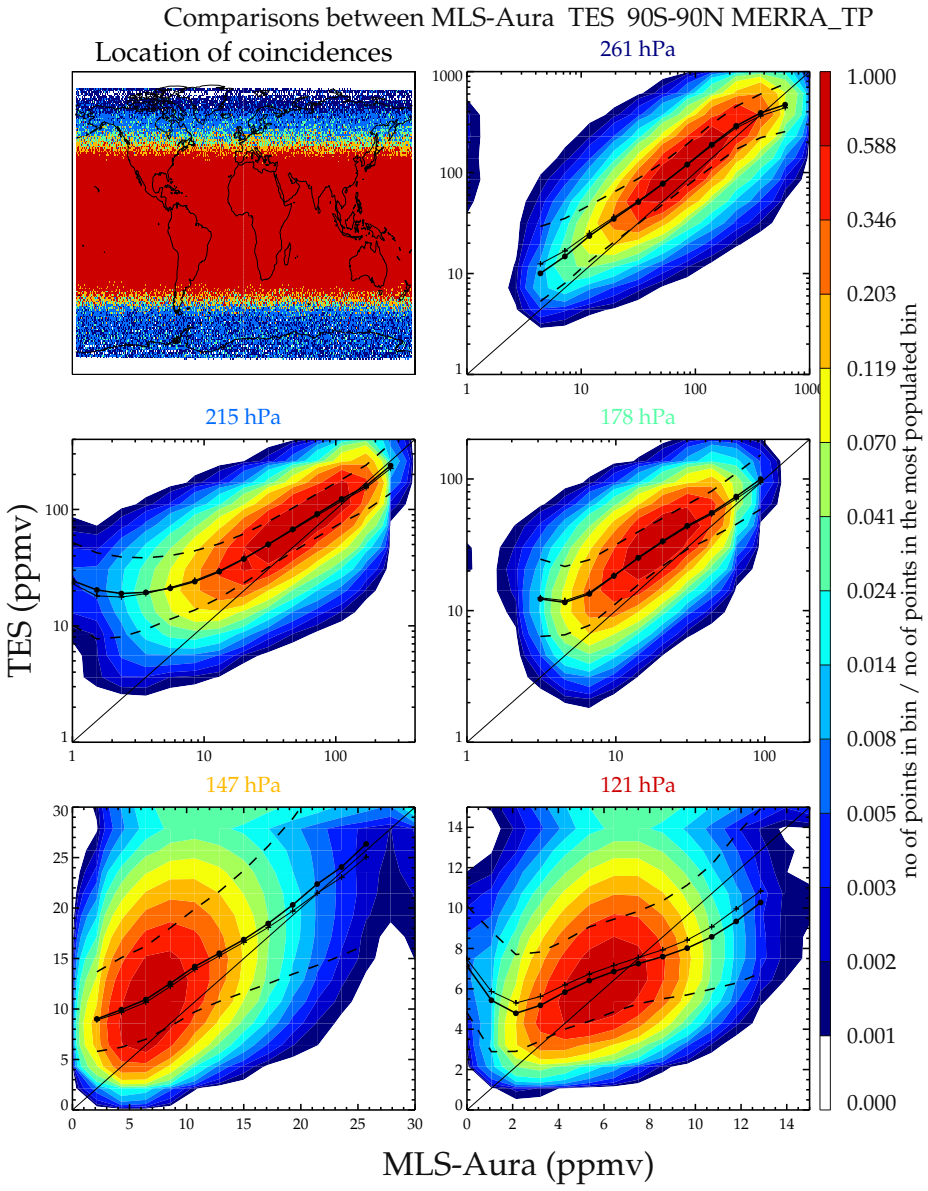

Figure S18. Scatter plot of coincident humidity measurements between MLS-Aura and TES

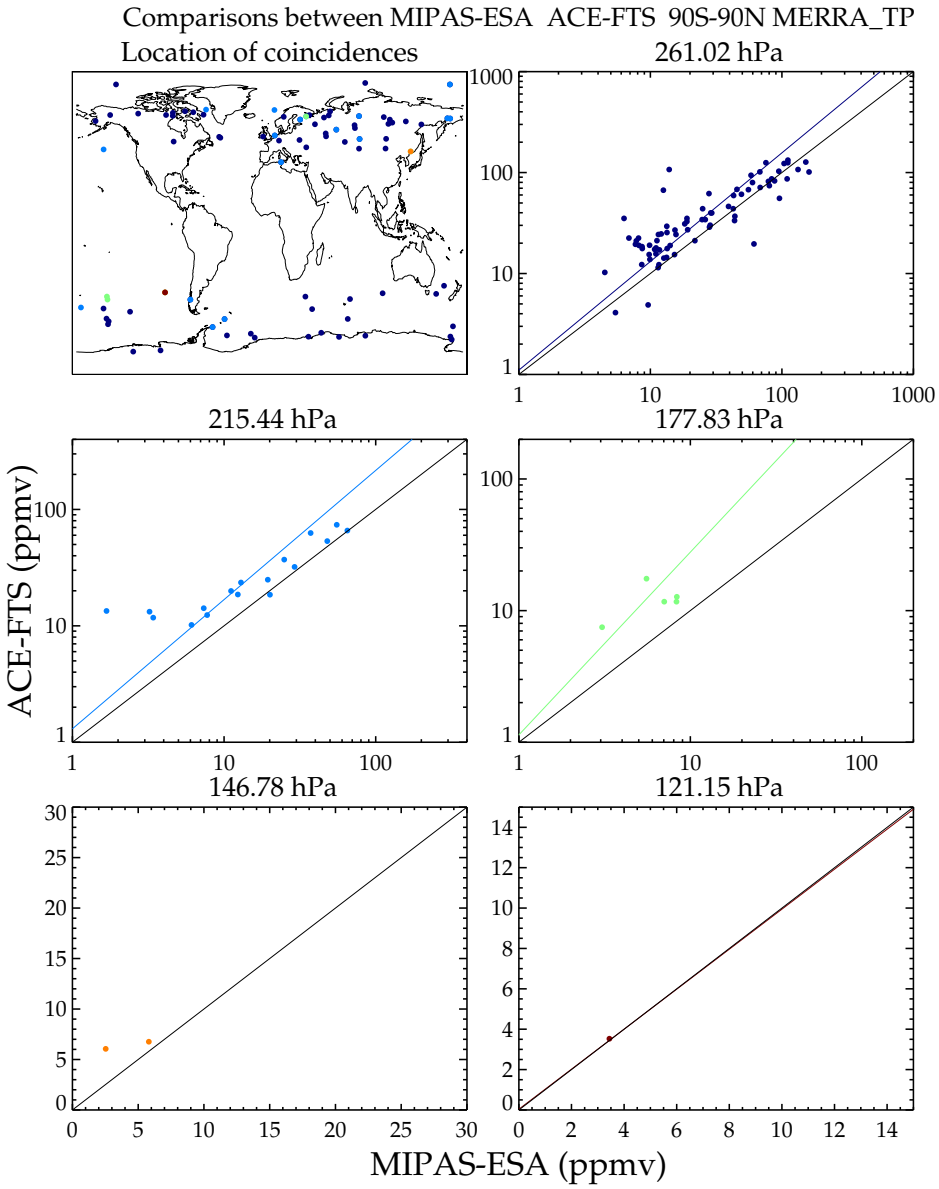

Figure S19. Scatter plot of coincident humidity measurements between MIPAS ESA and ACE-FTS

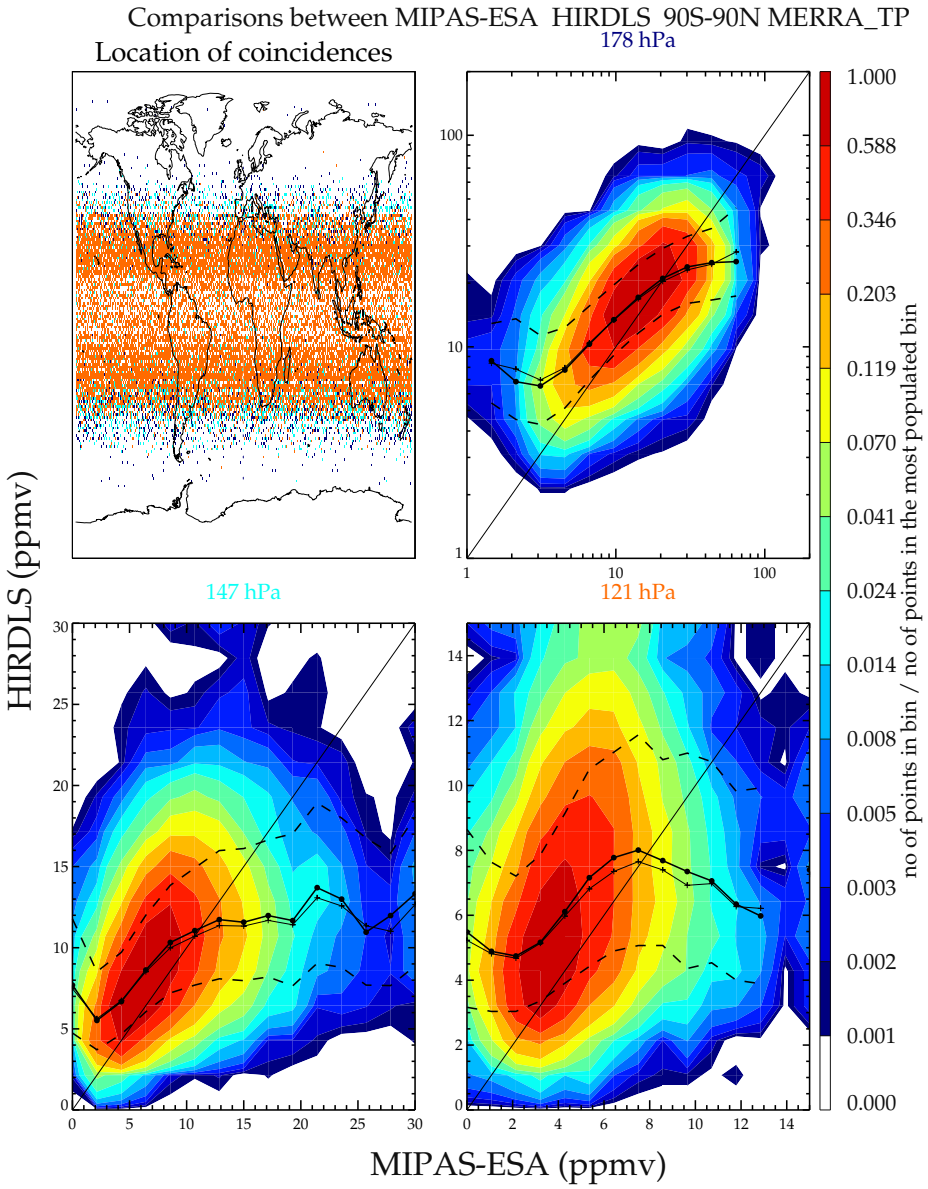

Figure S20. Scatter plot of coincident humidity measurements between MIPAS ESA and HIRDLS

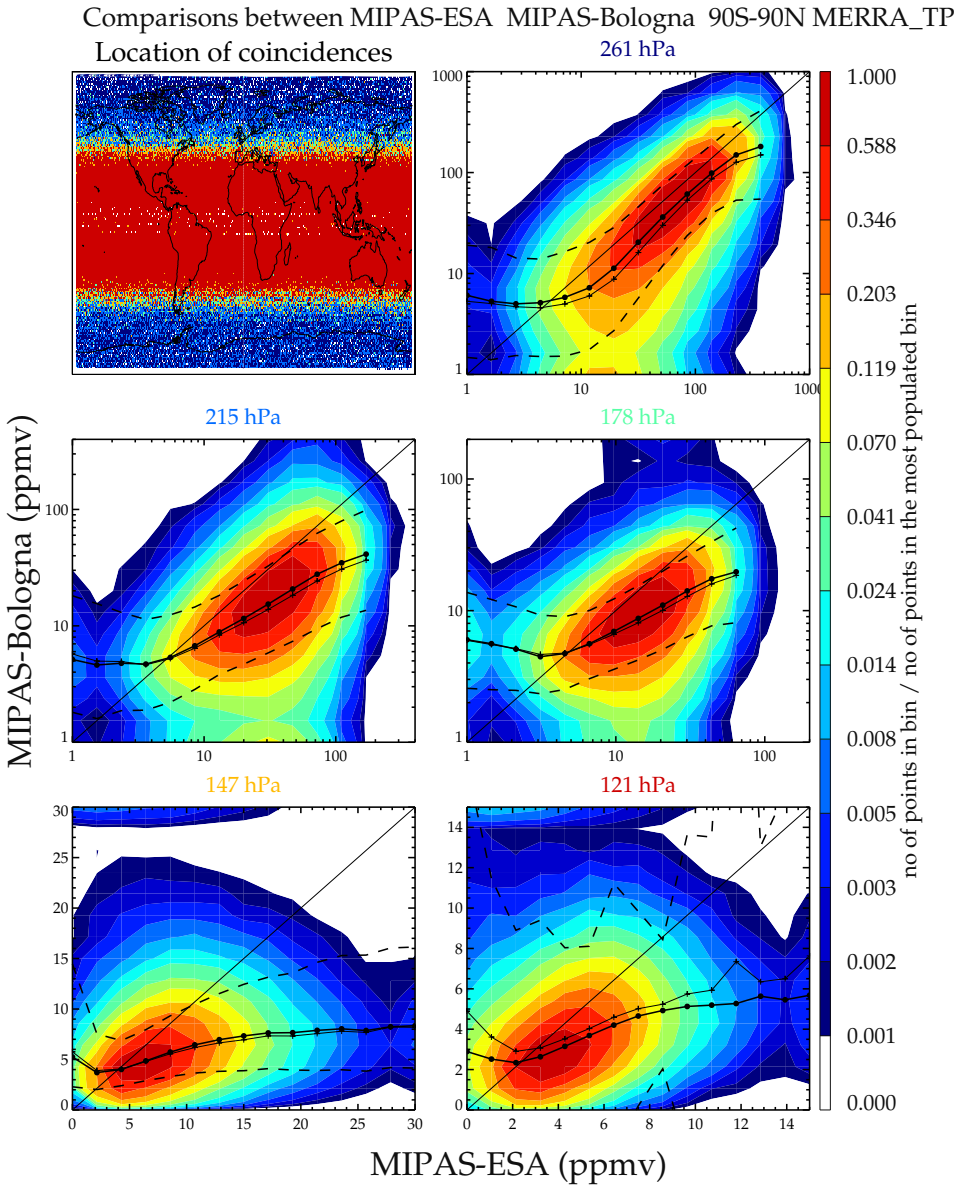

Figure S21. Scatter plot of coincident humidity measurements between MIPAS ESA and MIPAS Bologna

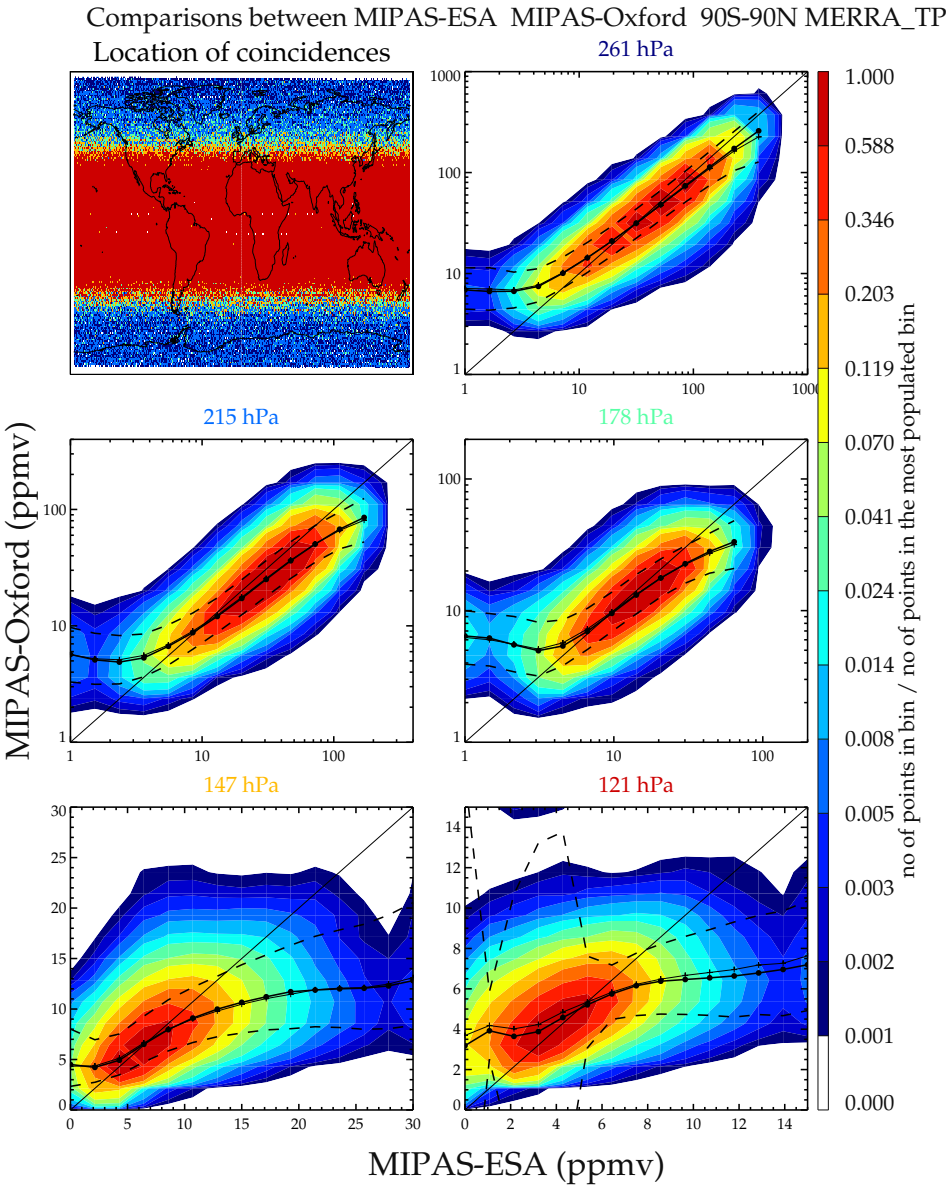

Figure S22. Scatter plot of coincident humidity measurements between MIPAS ESA and MIPAS Oxford

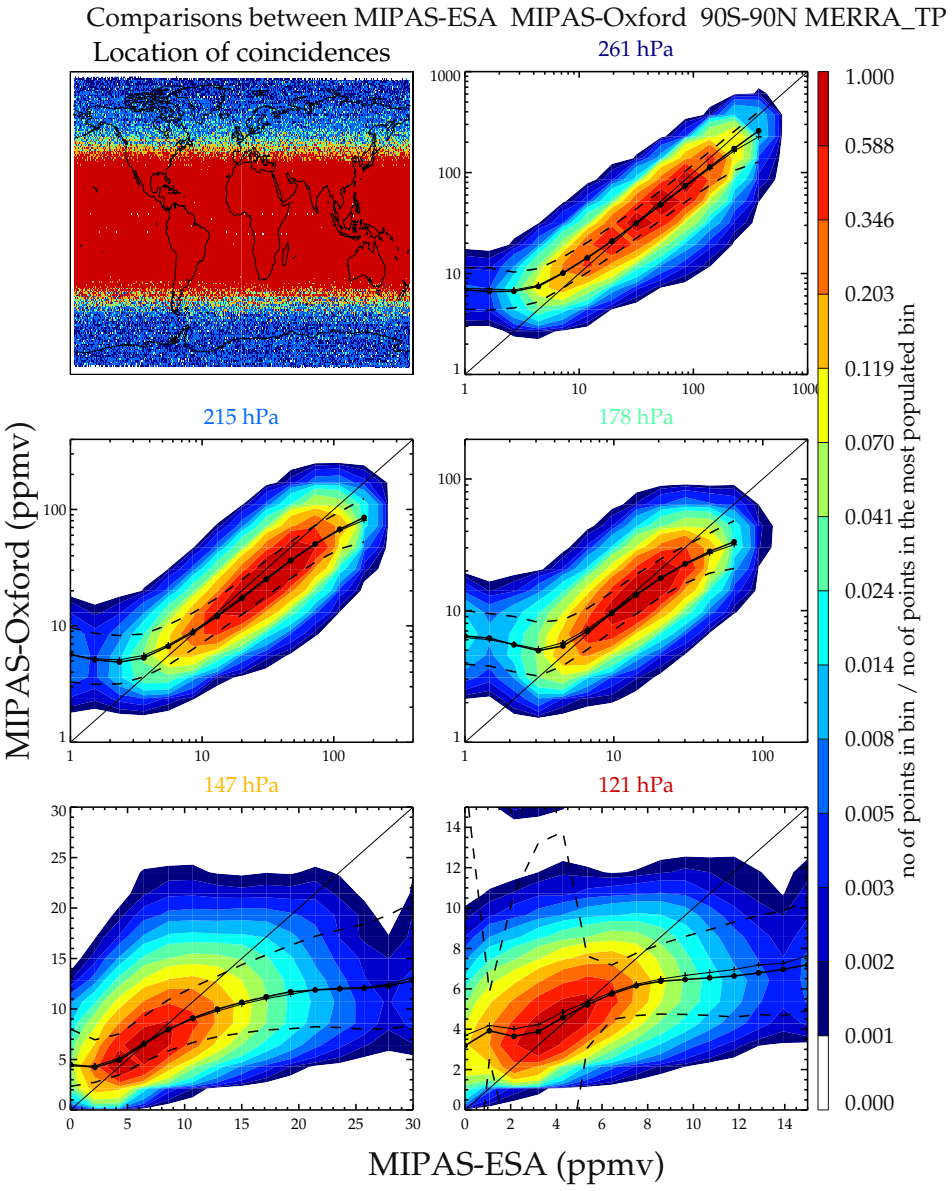

Figure S23. Scatter plot of coincident humidity measurements between MIPAS ESA and MIPAS Oxford

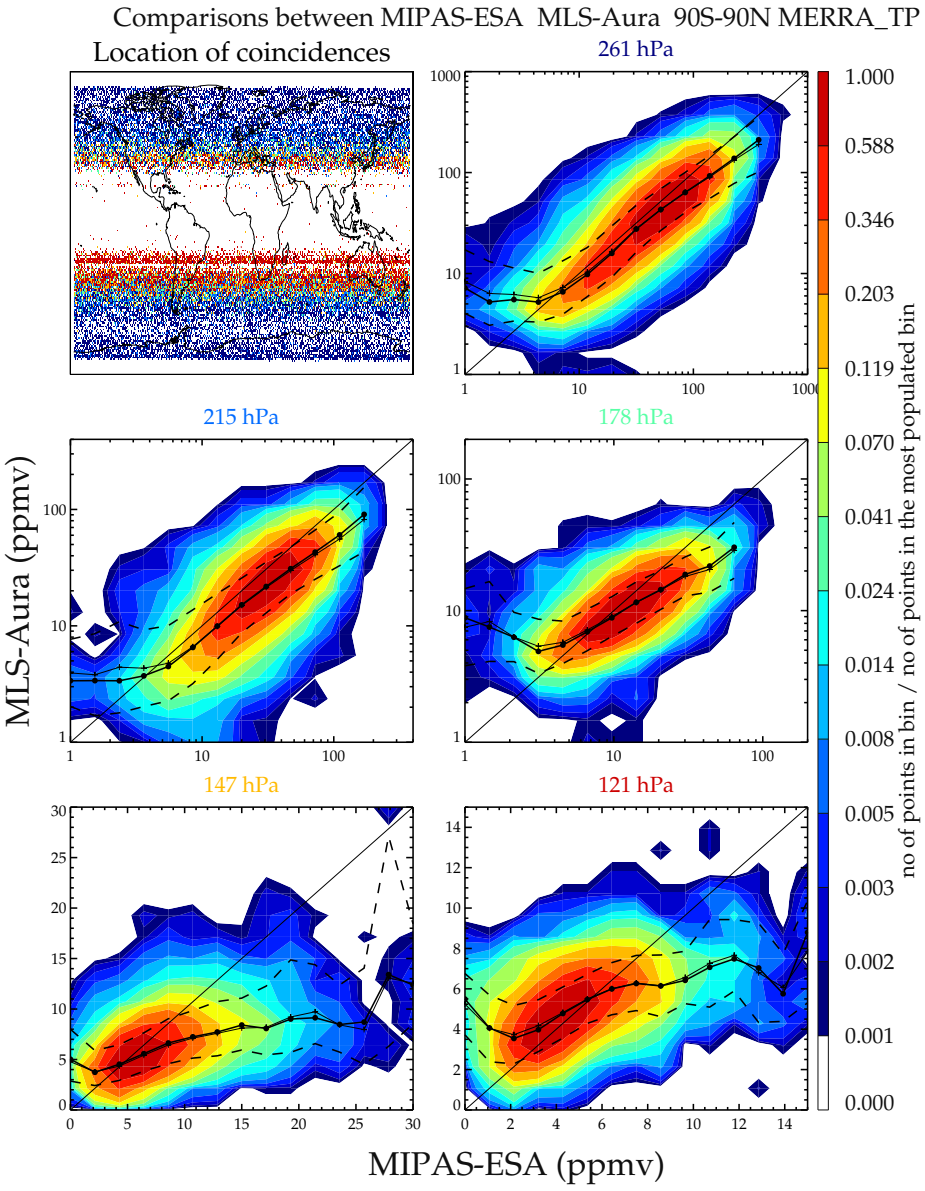

Figure S24. Scatter plot of coincident humidity measurements between MIPAS ESA and MLS Aura

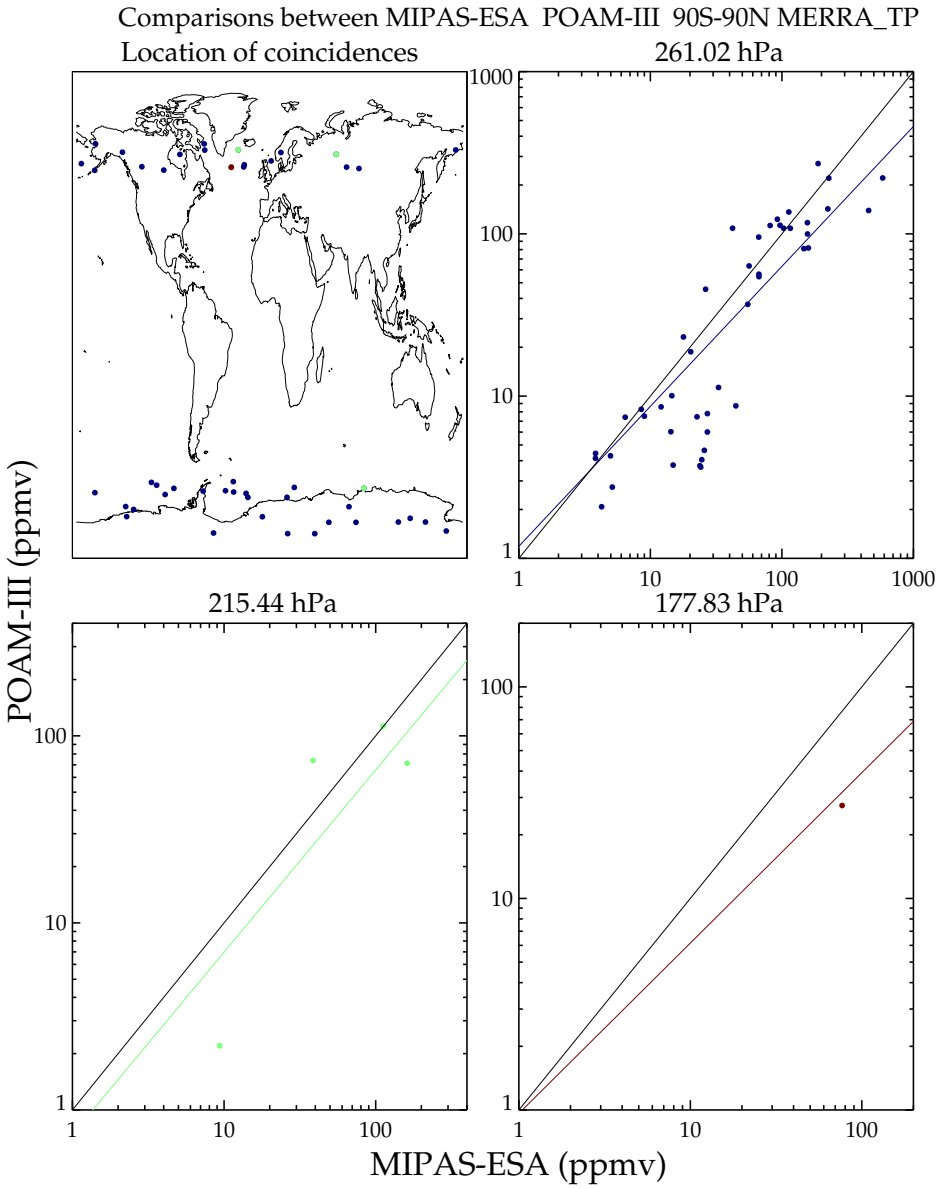

Figure S25. Scatter plot of coincident humidity measurements between MIPAS ESA and POAM-III

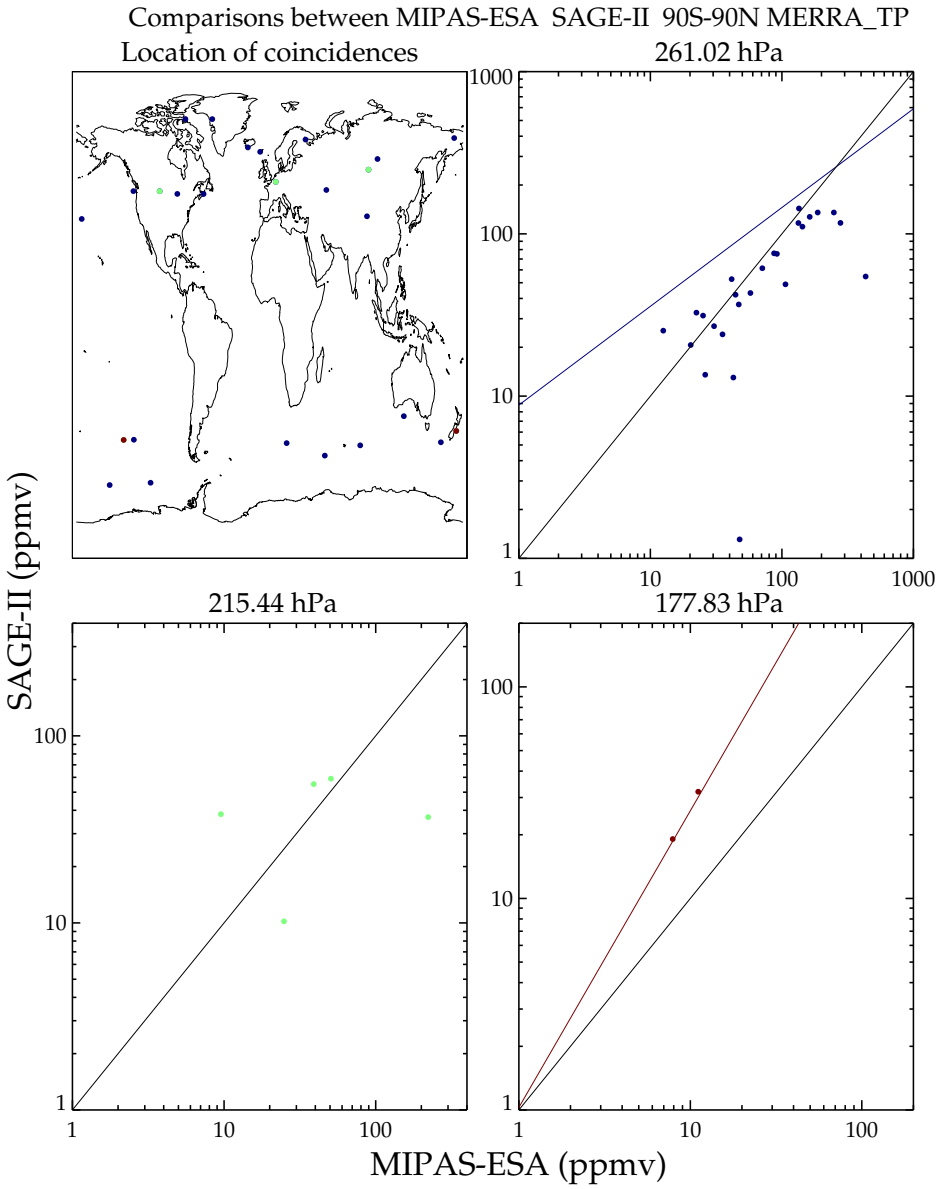

Figure S26. Scatter plot of coincident humidity measurements between MIPAS ESA and SAGE-II

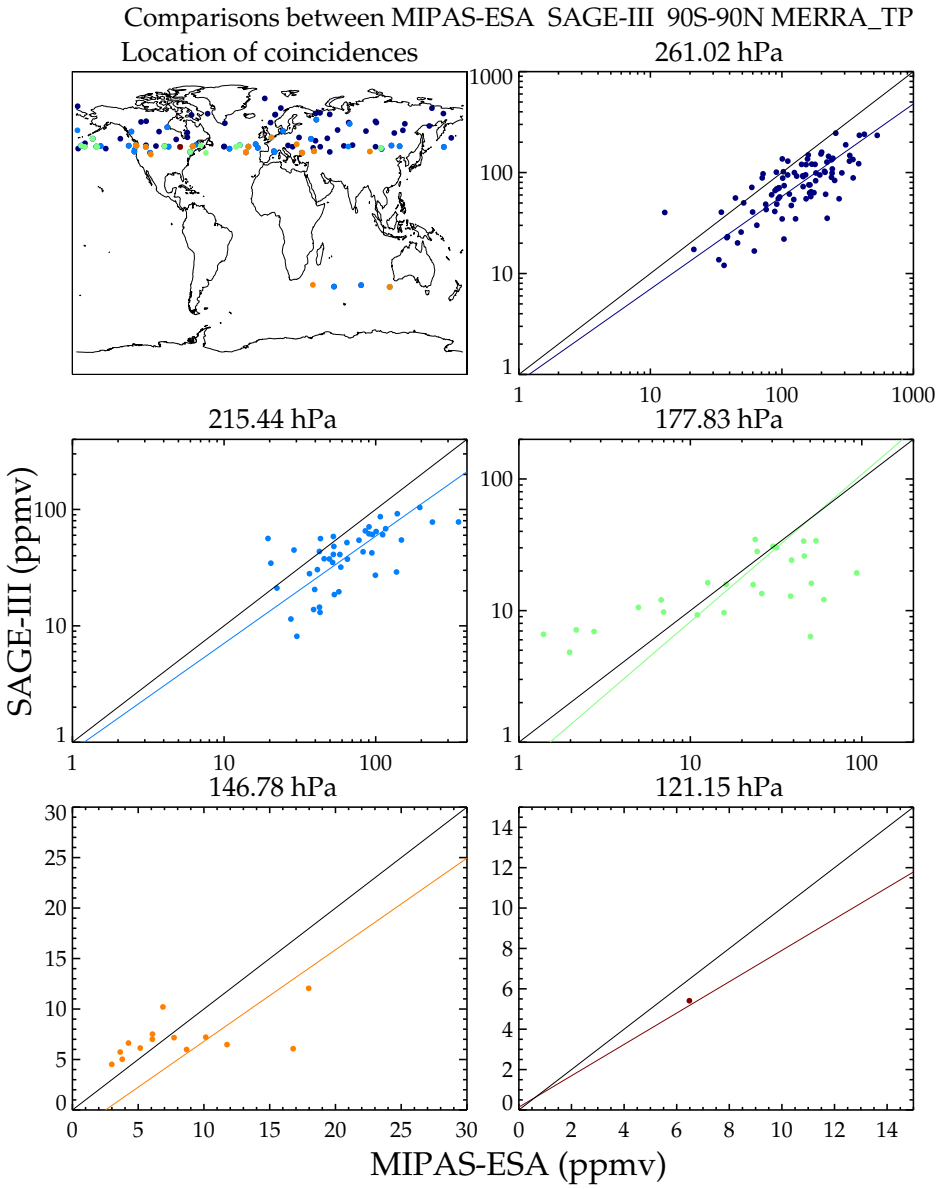

Figure S27. Scatter plot of coincident humidity measurements between MIPAS ESA and SAGE-III

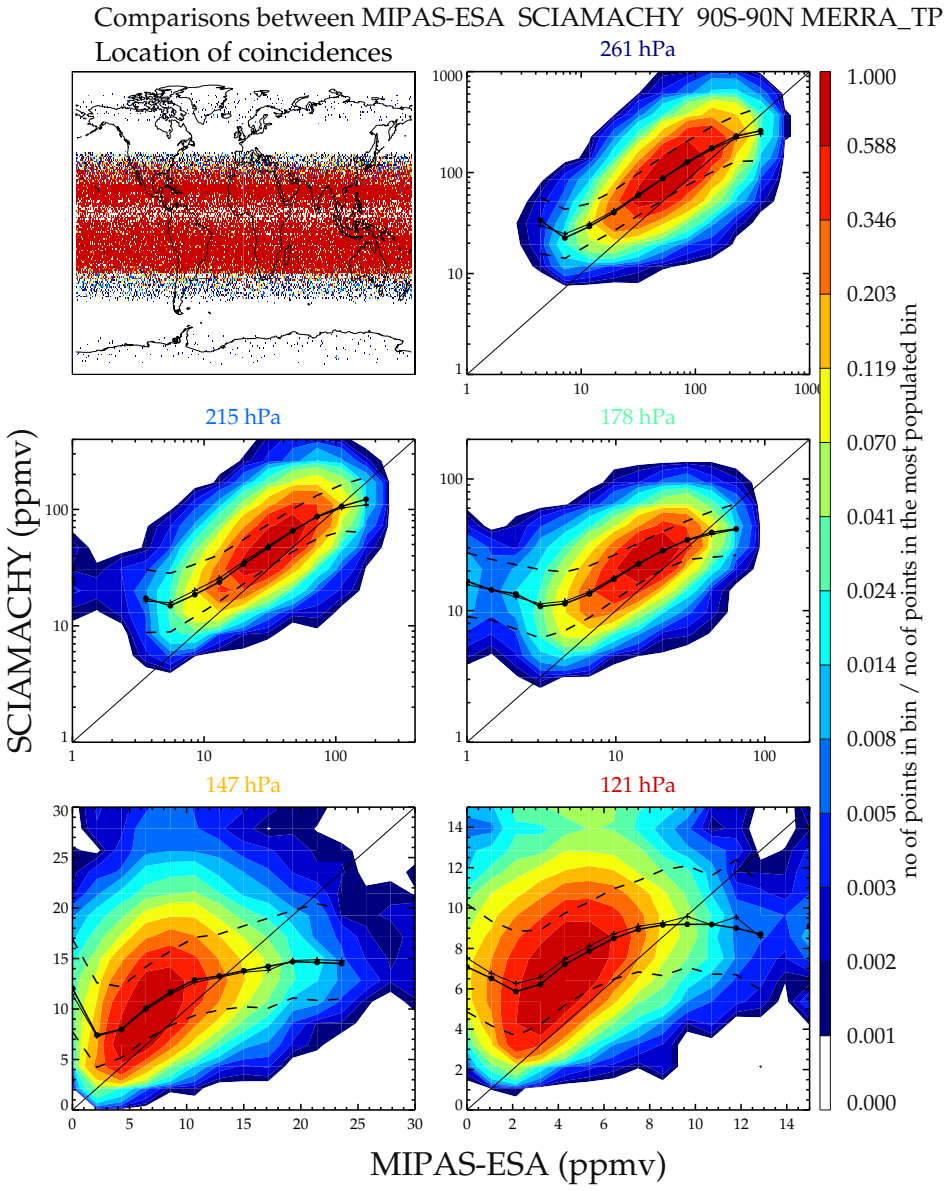

Figure S28. Scatter plot of coincident humidity measurements between MIPAS ESA and SCIAMACHY

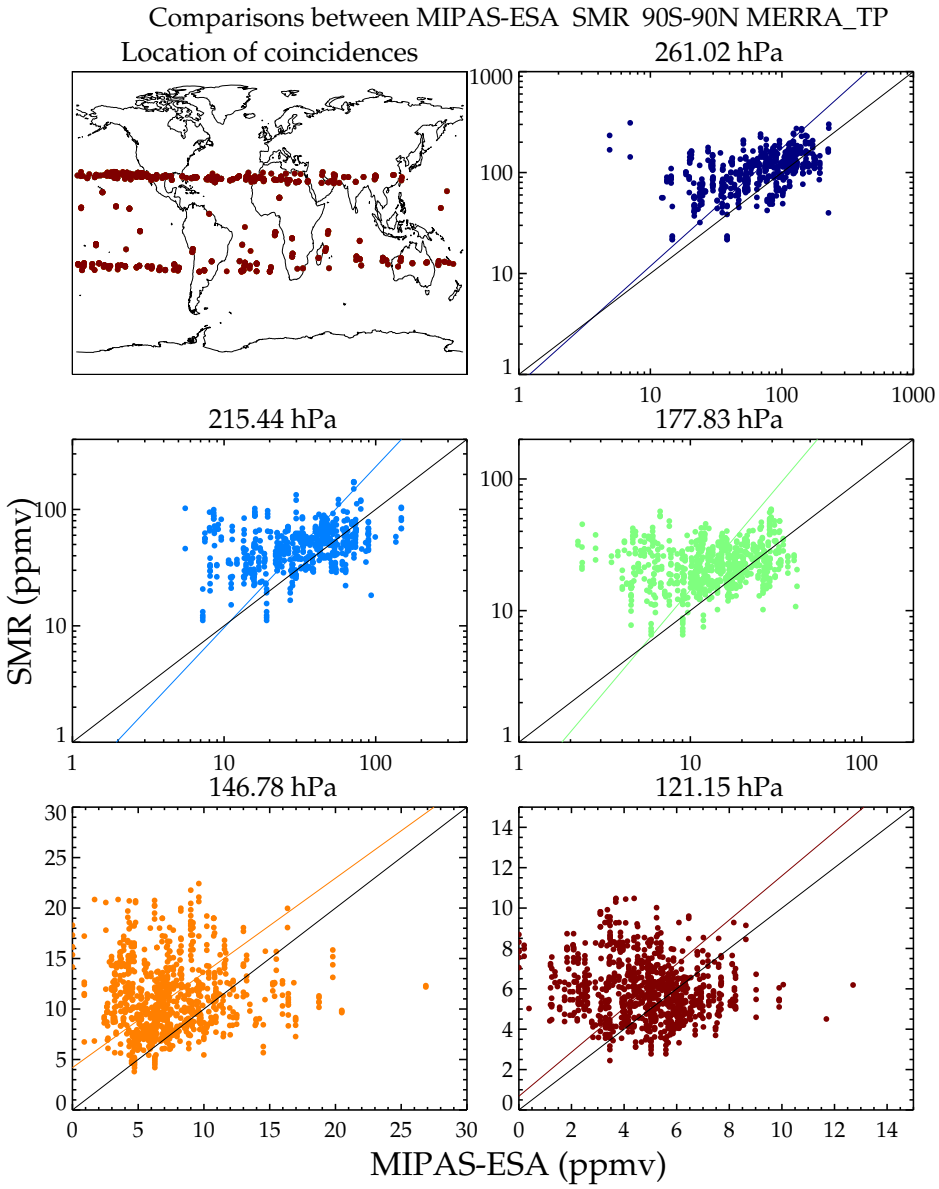

Figure S29. Scatter plot of coincident humidity measurements between MIPAS ESA and SMR

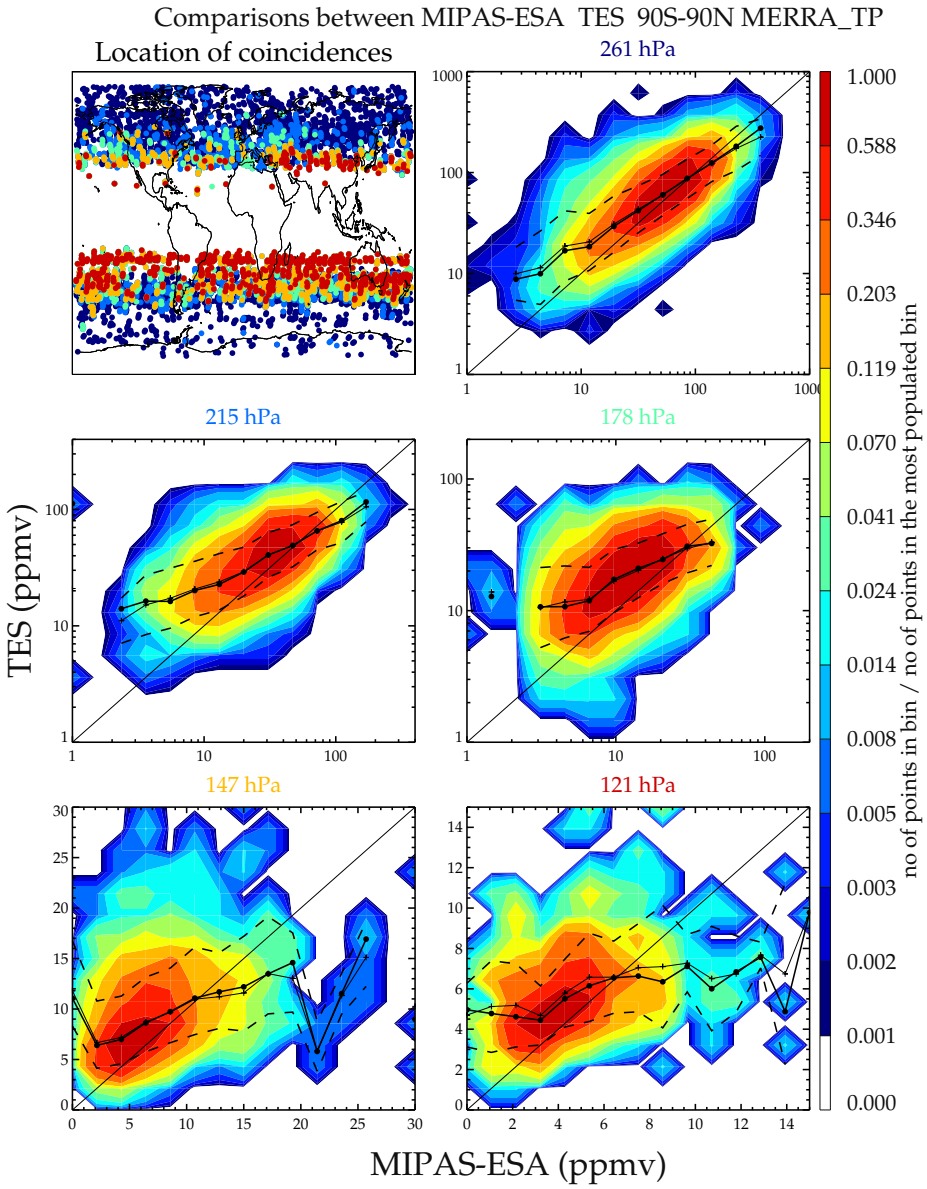

Figure S30. Scatter plot of coincident humidity measurements between MIPAS ESA and TES

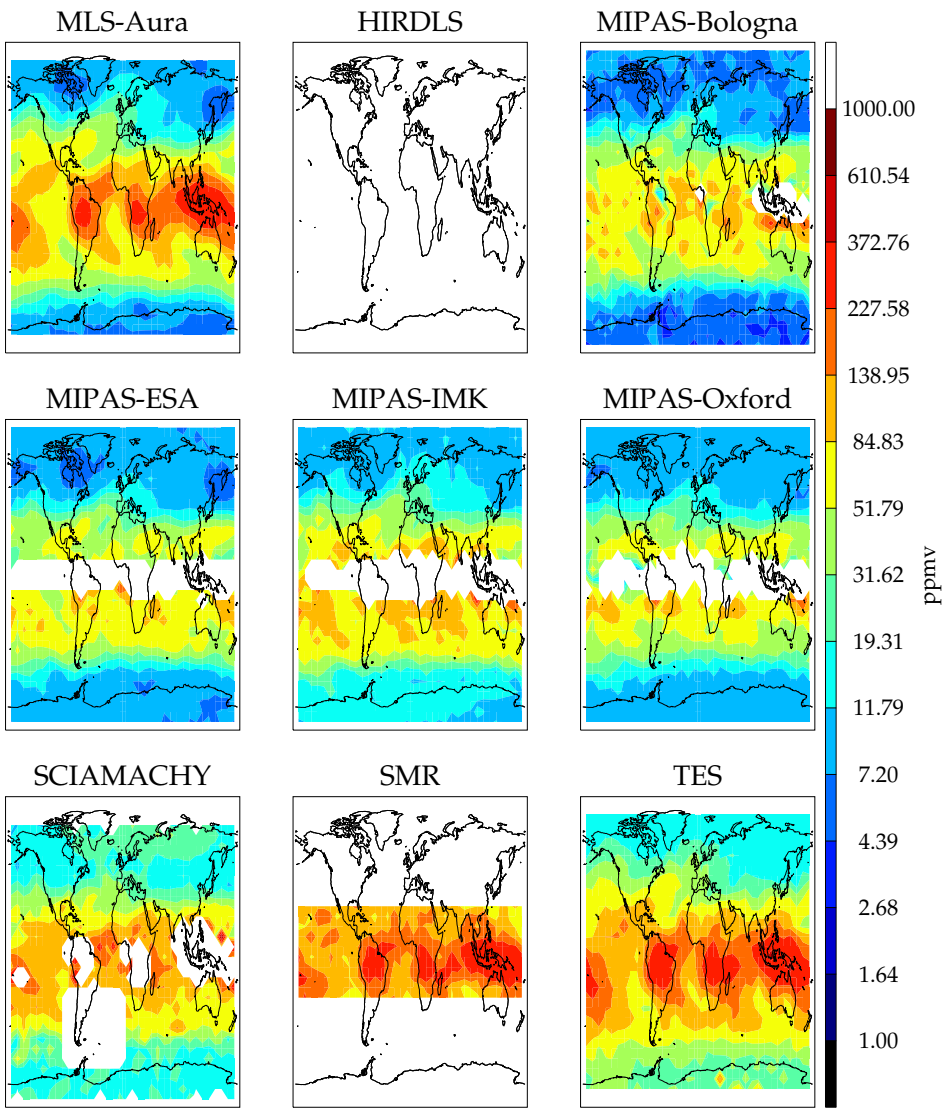

Figure S31. Gridded maps for nine instruments at 250 hPa.

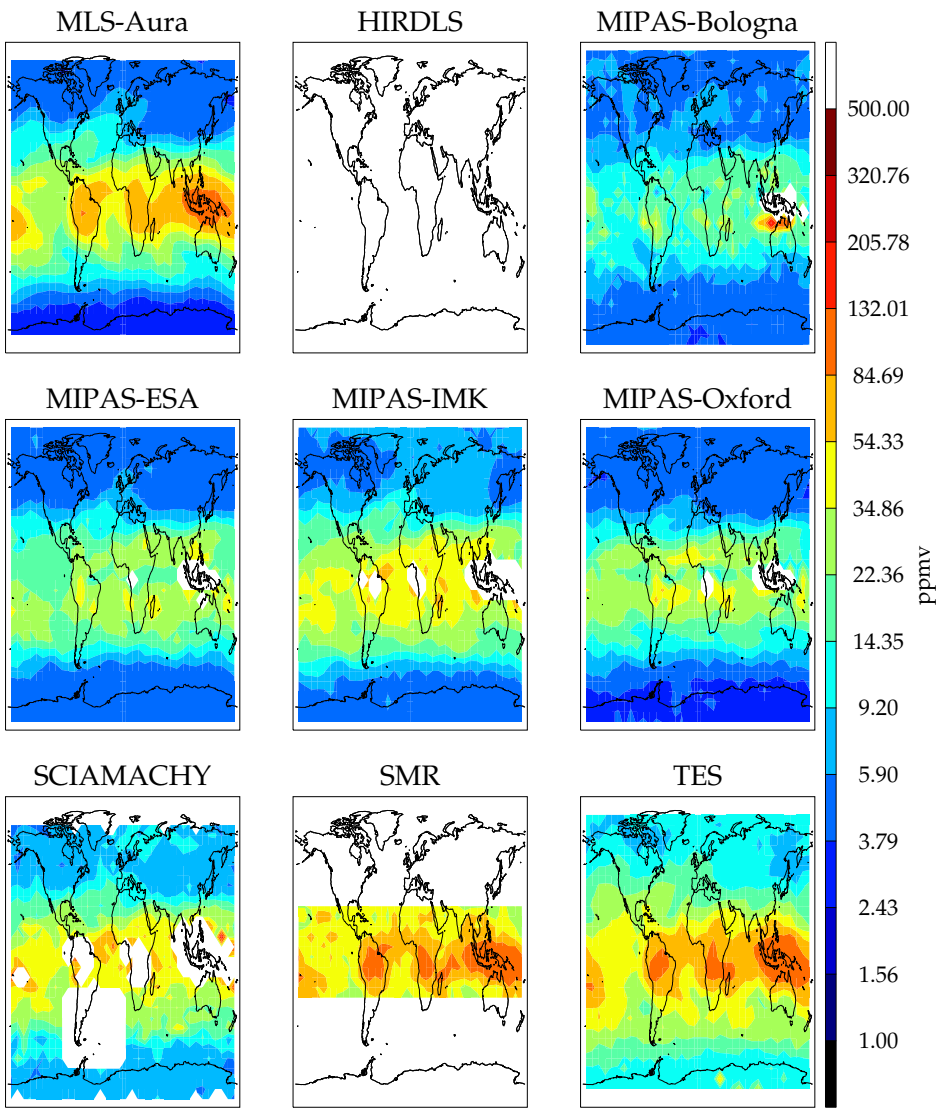

Figure S32. Gridded maps for nine instruments at 200 hPa.

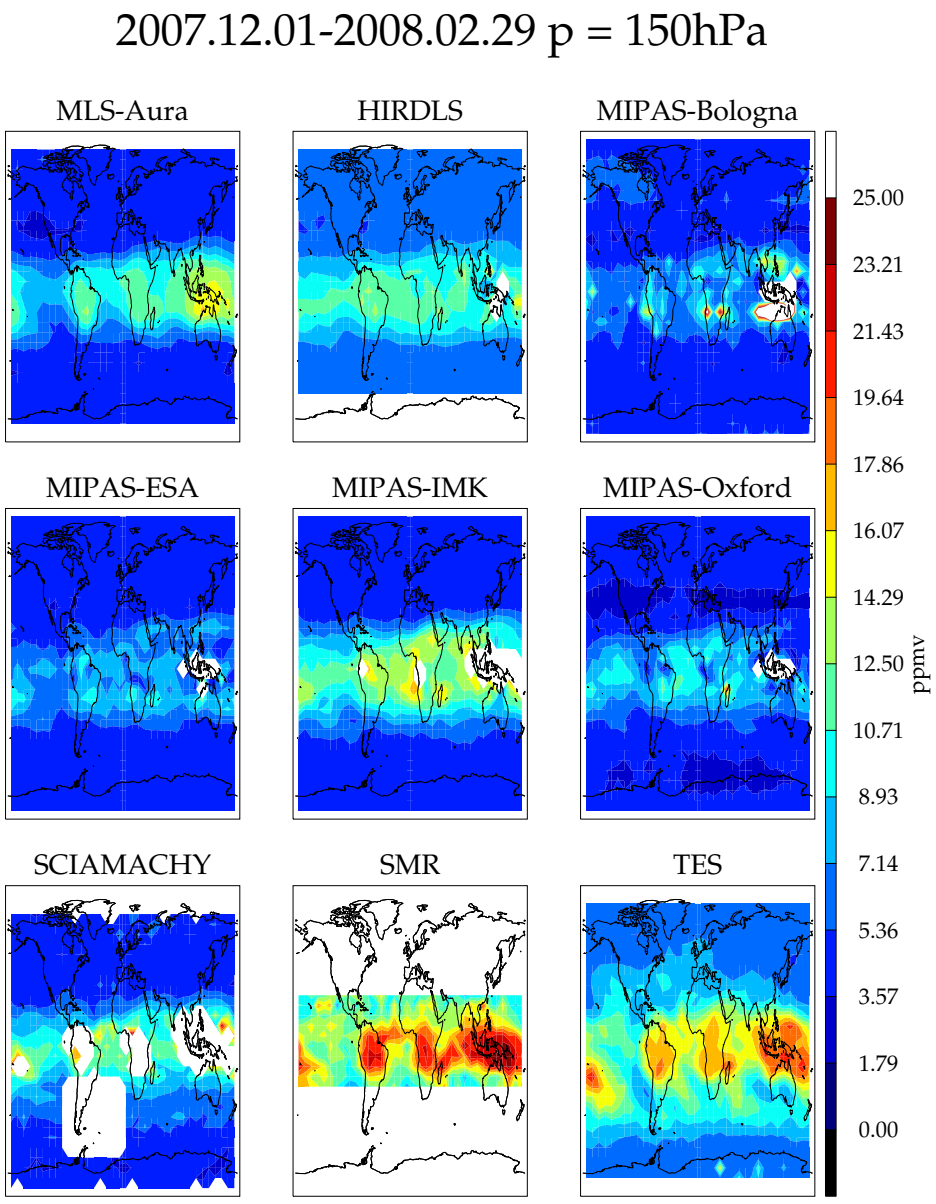

Figure S33. Gridded maps for nine instruments at 150 hPa.

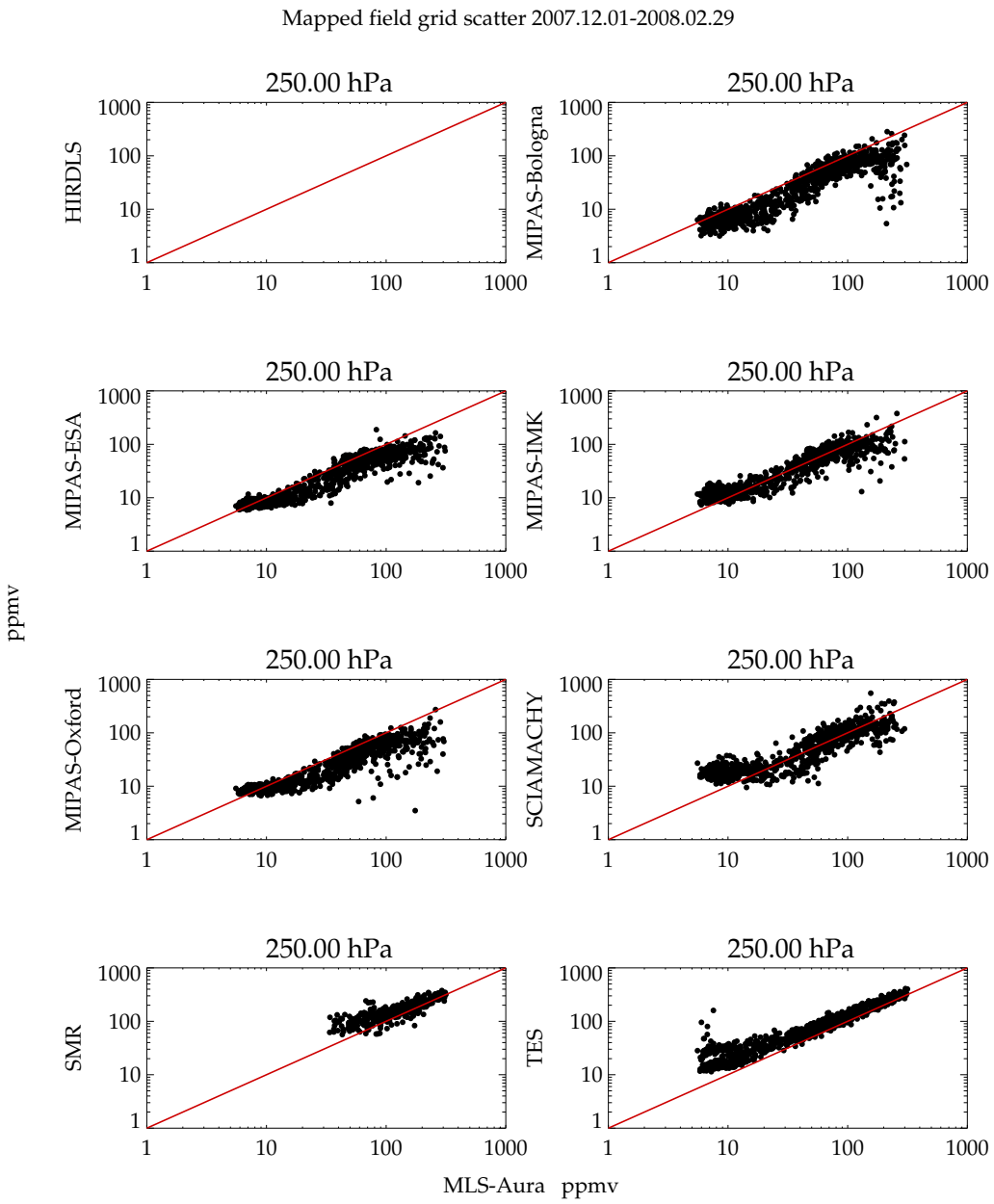

Figure S34. Scatter plot of mapped grid box values of 8 instruments versus MLS Aura at 250 hPa.

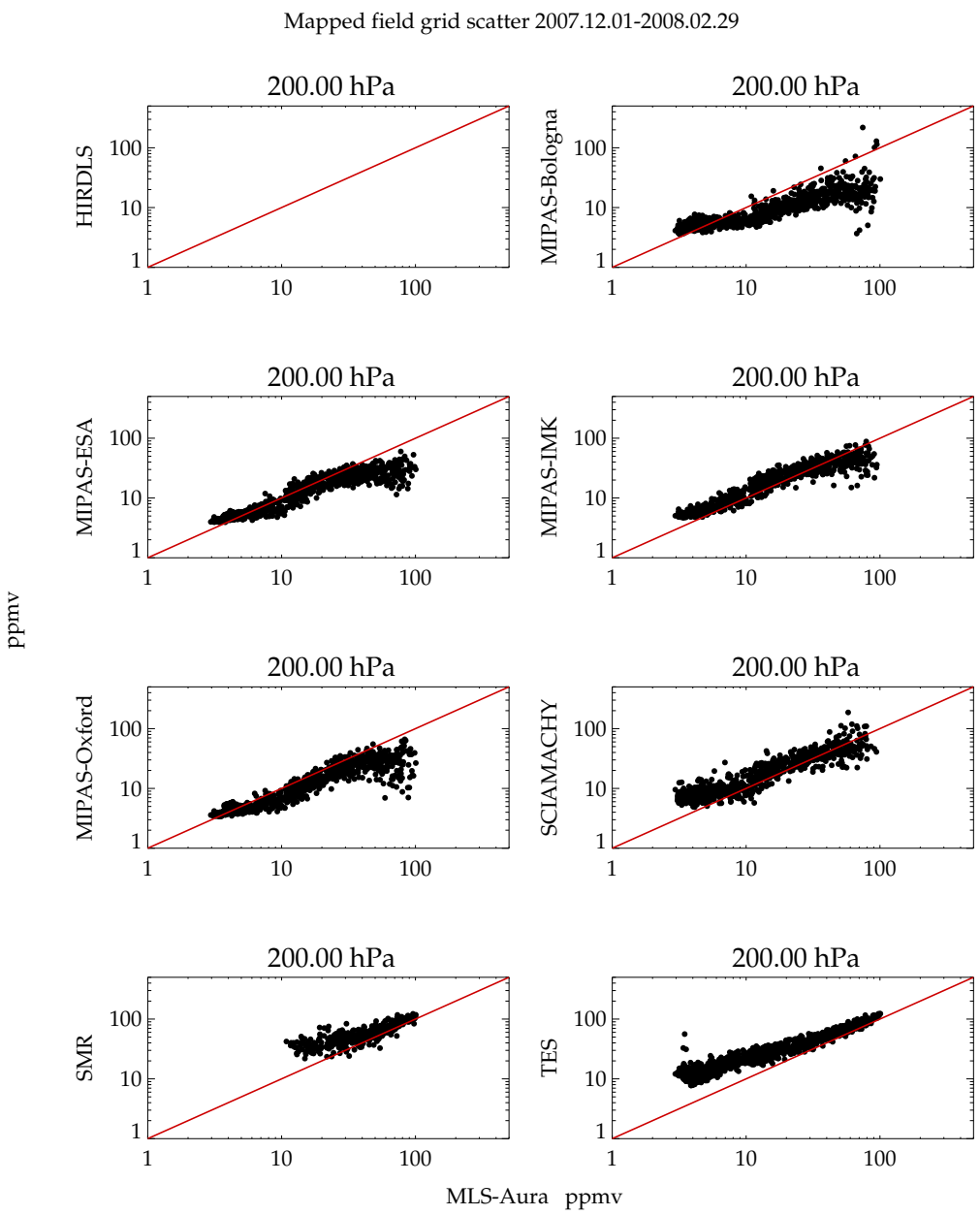

Figure S35. Scatter plot of mapped grid box values of 8 instruments versus MLS Aura at 200 hPa.

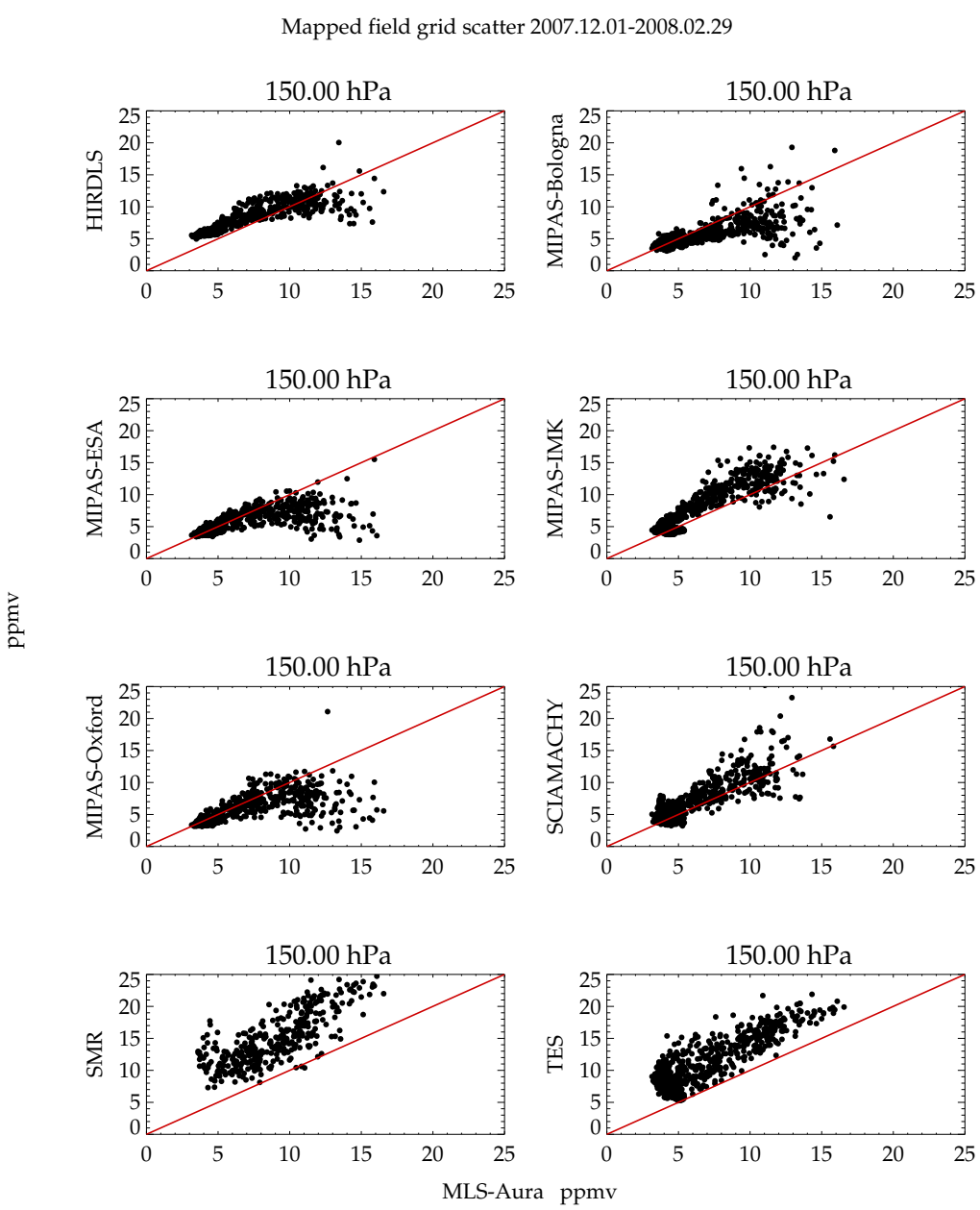

Figure S36. Scatter plot of mapped grid box values of 8 instruments versus MLS Aura at 150 hPa.

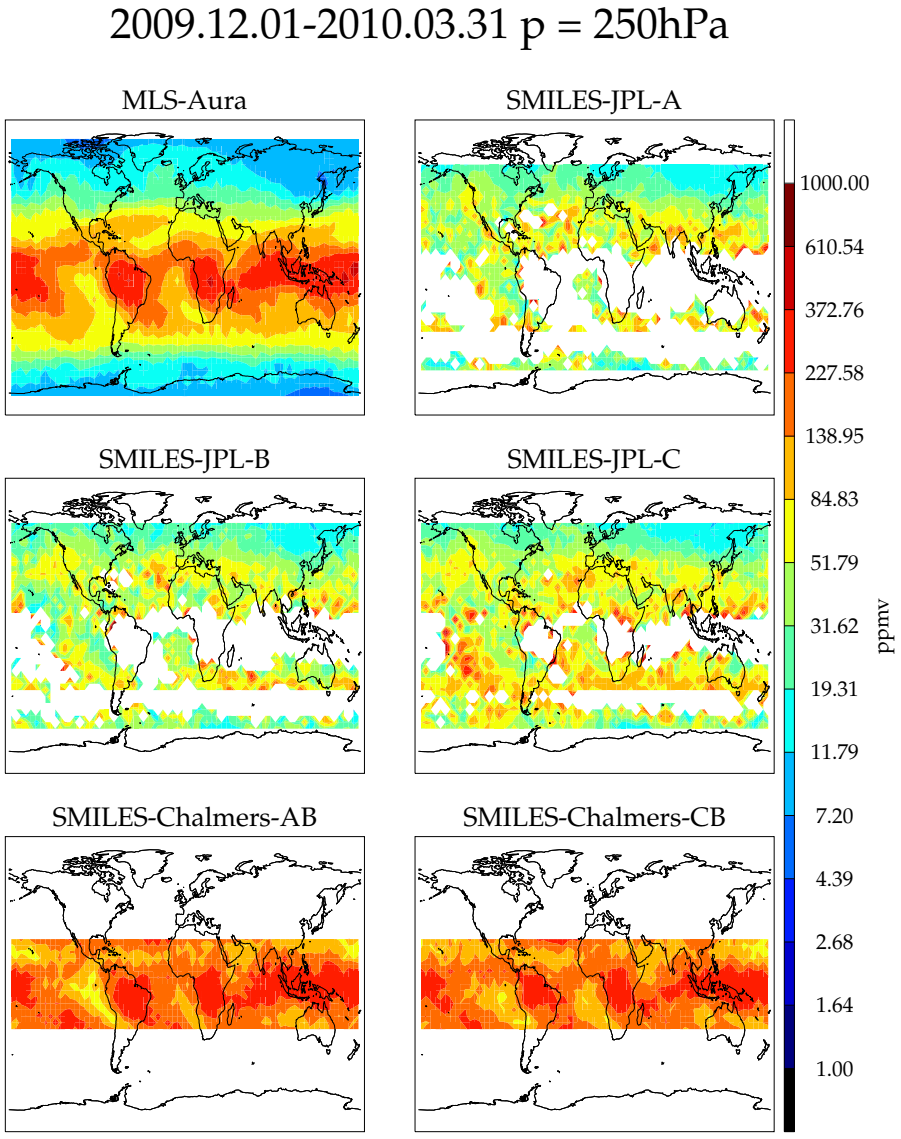

Figure S37. Gridded maps for SMILES humidity retrieval products at 250 hPa.

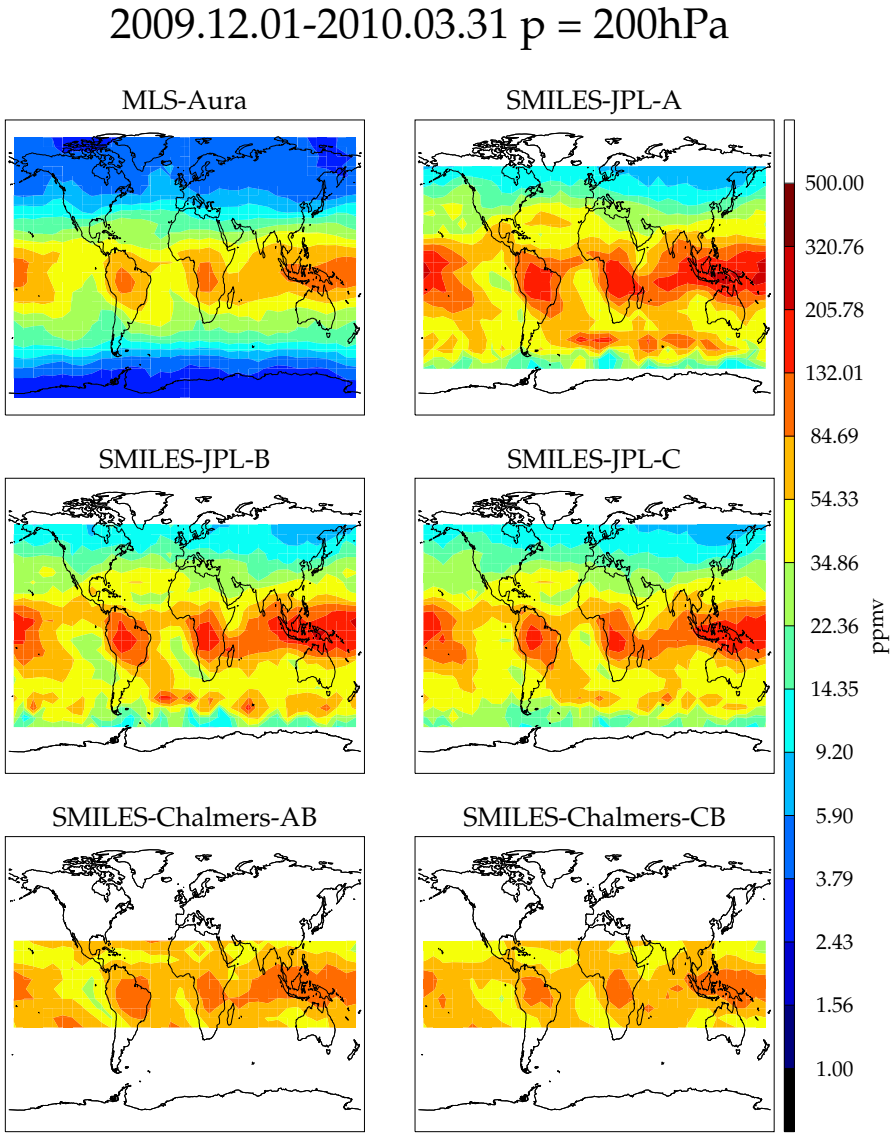

Figure S38. Gridded maps for SMILES humidity retrieval products at 200 hPa.

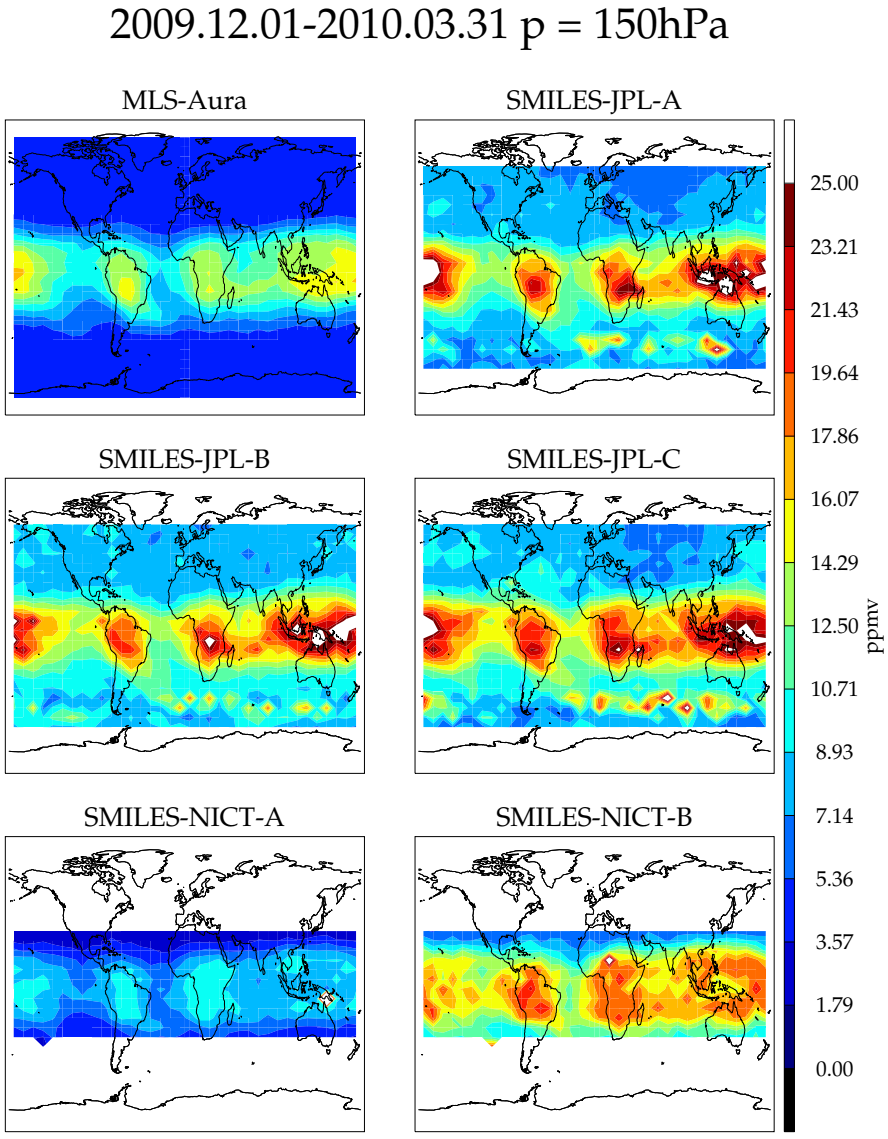

Figure S39. Gridded maps for SMILES humidity retrieval products at 150 hPa.

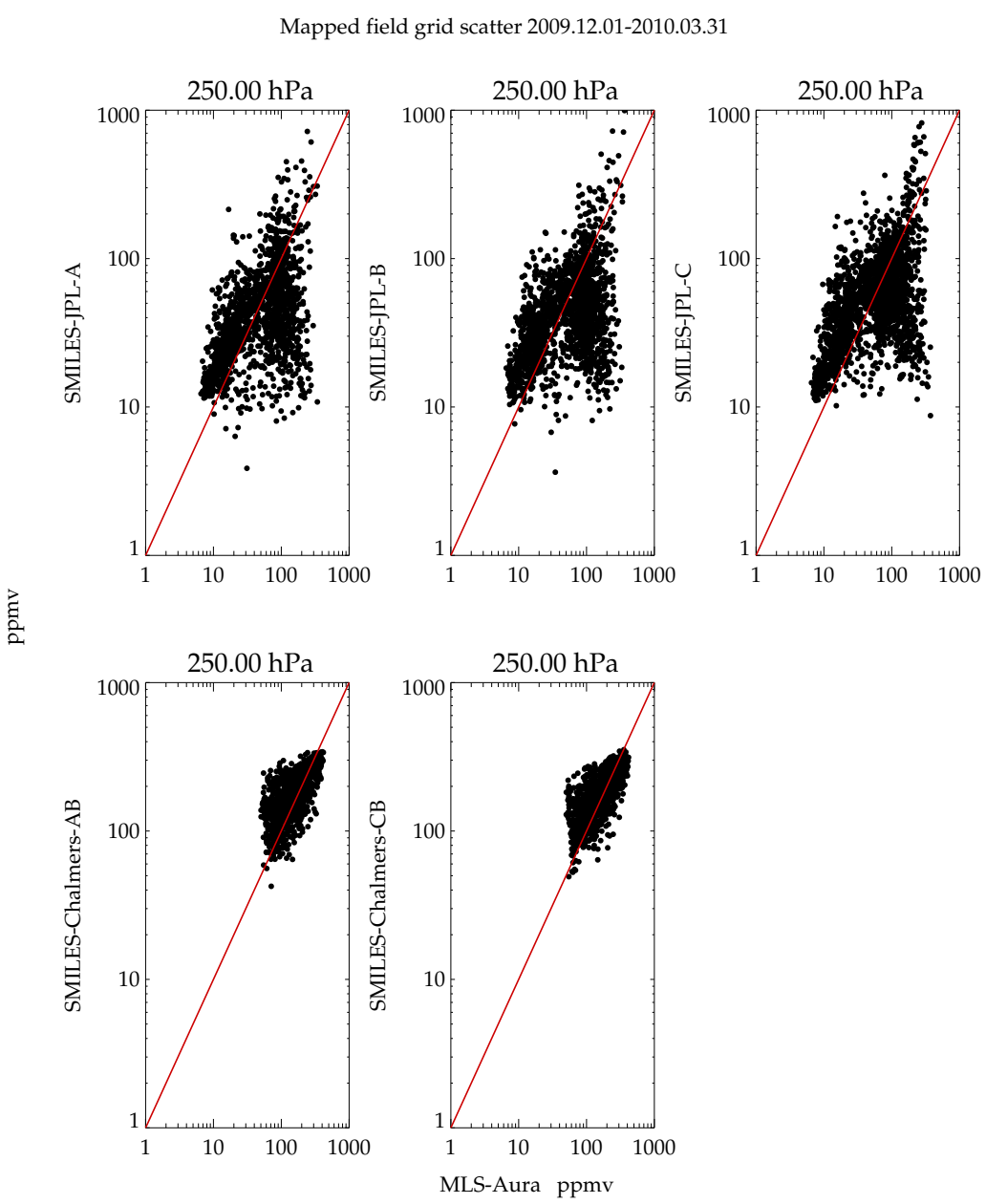

Figure S40. Scatter plot of mapped grid box values of SMILES humidity retrievals versus MLS Aura at 250 hPa.

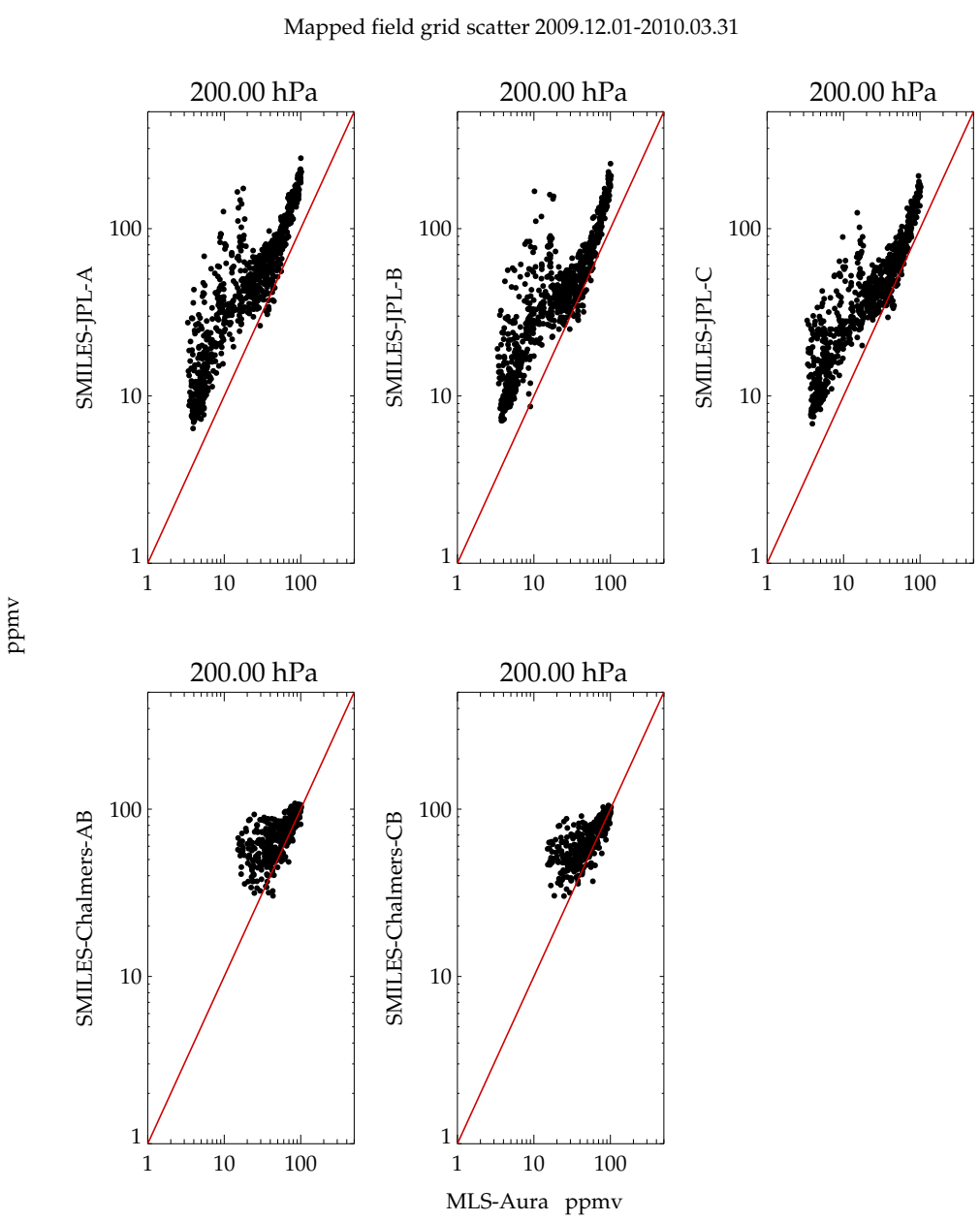

Figure S41. Scatter plot of mapped grid box values of SMILES humidity retrievals versus MLS Aura at 200 hPa.

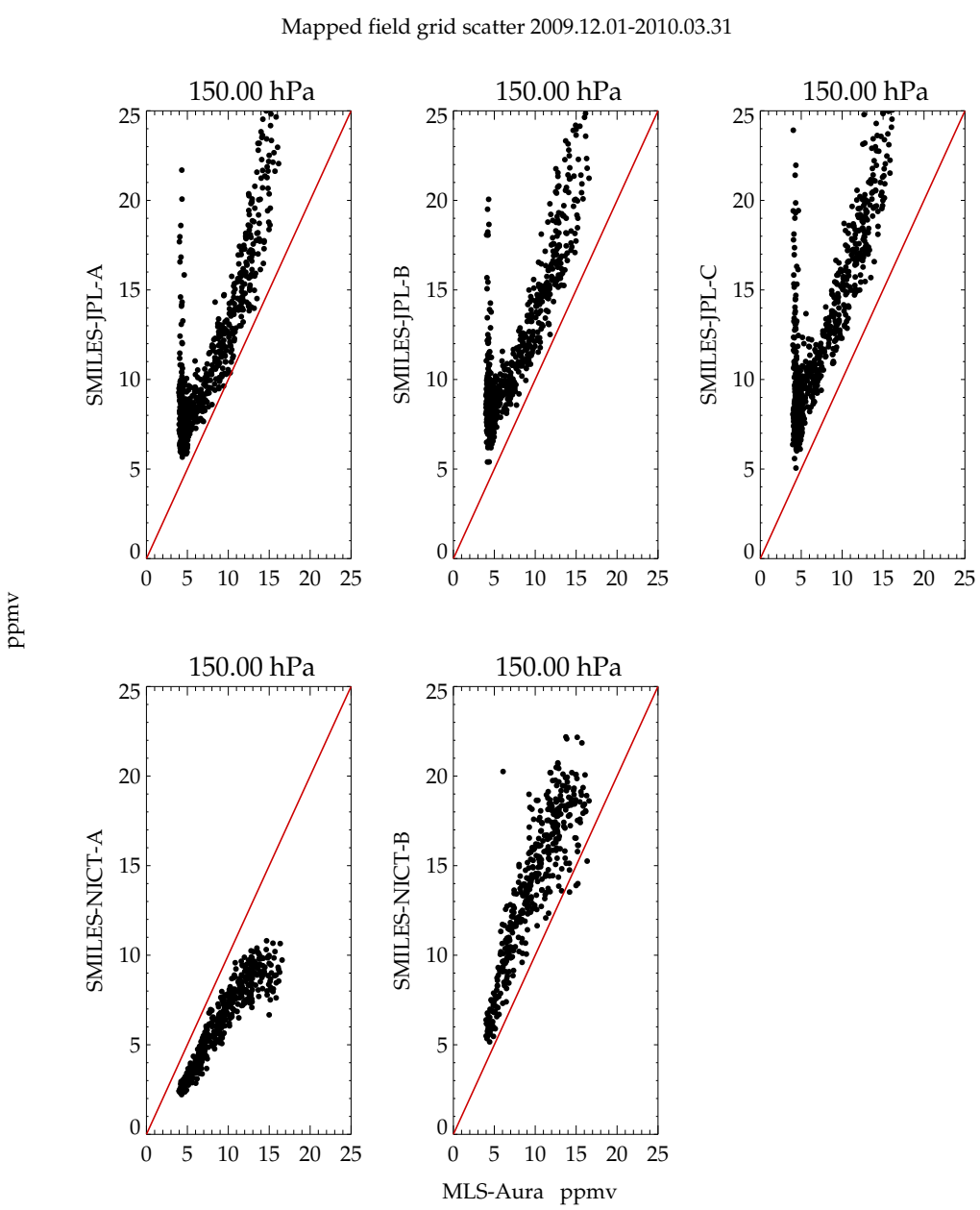

Figure S42. Scatter plot of mapped grid box values of SMILES humidity retrievals versus MLS Aura at 150 hPa.

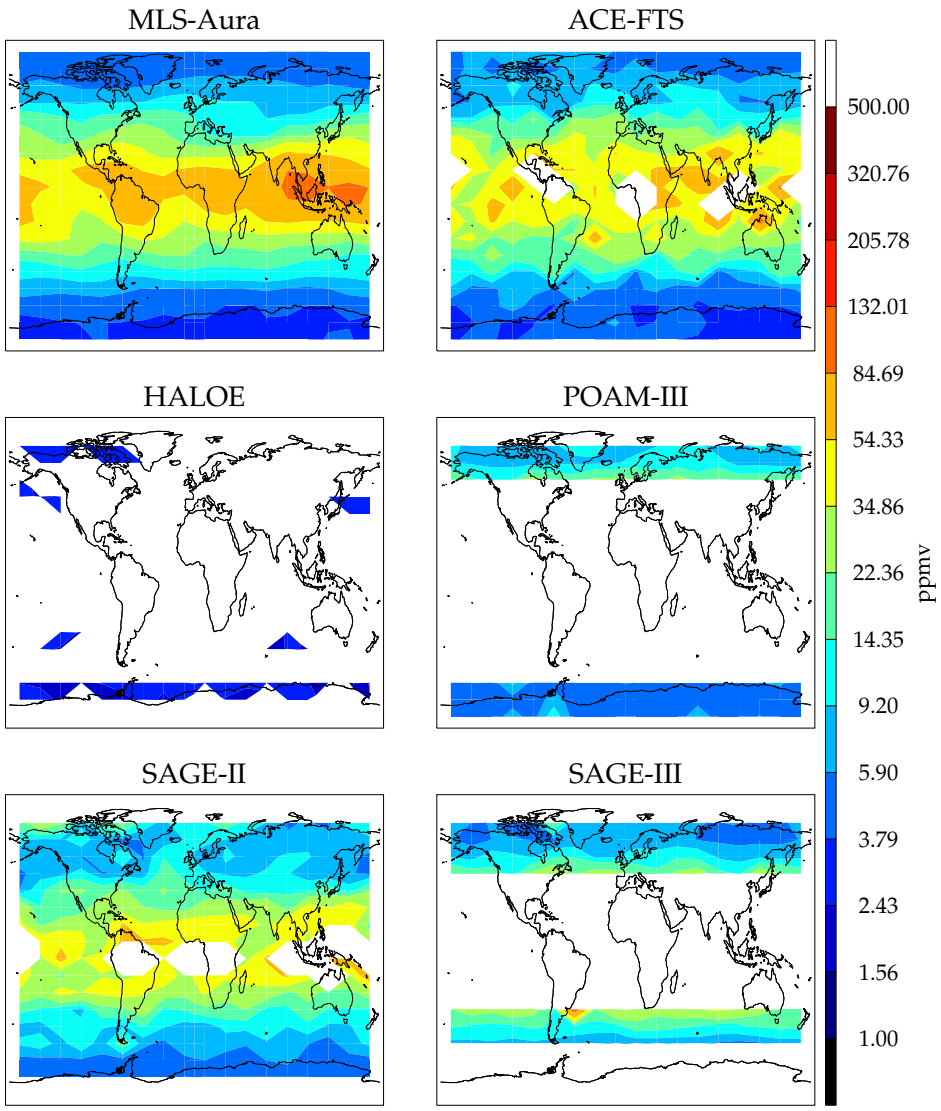

Figure S43. Gridded maps for occultation humidity retrieval products at 200 hPa.

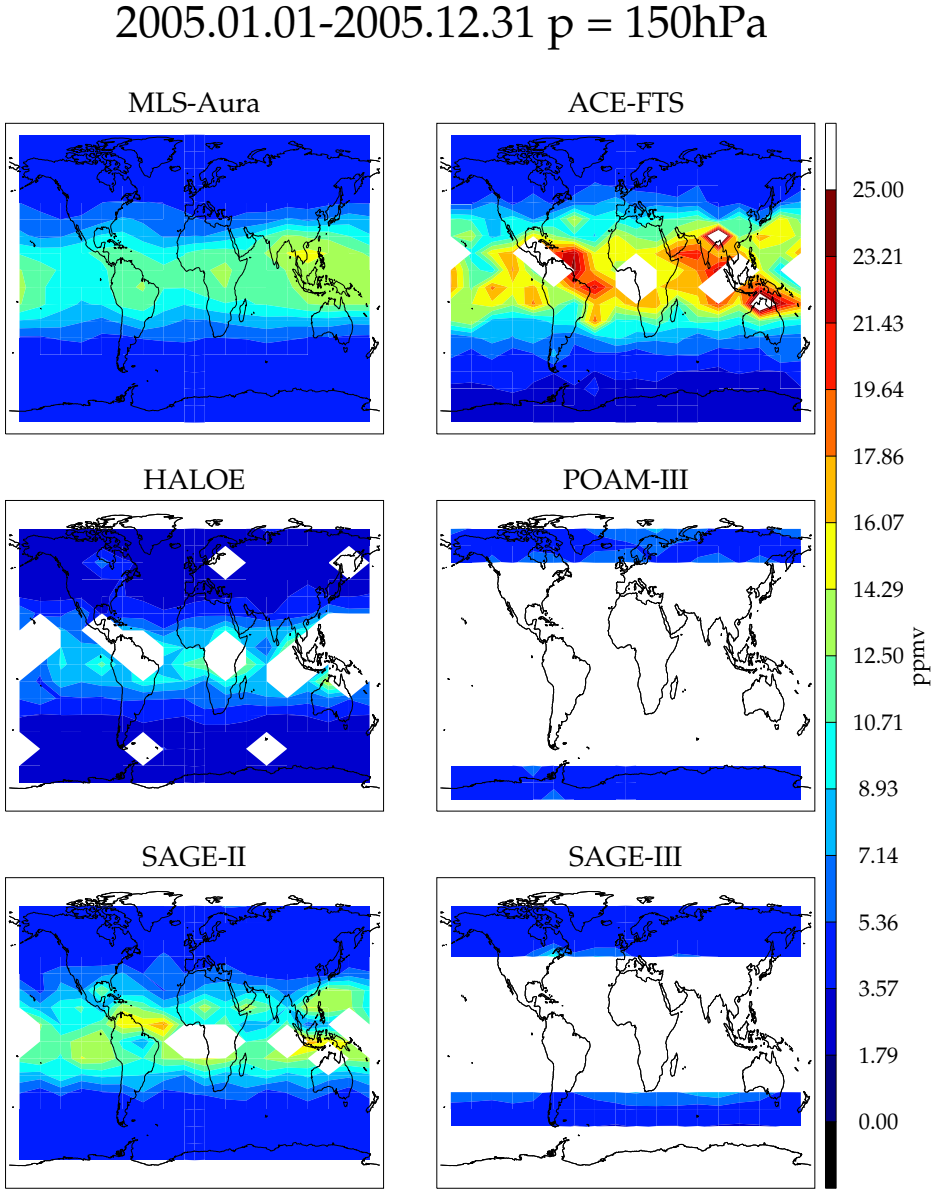

Figure S44. Gridded maps for occultation humidity retrieval products at 150 hPa.

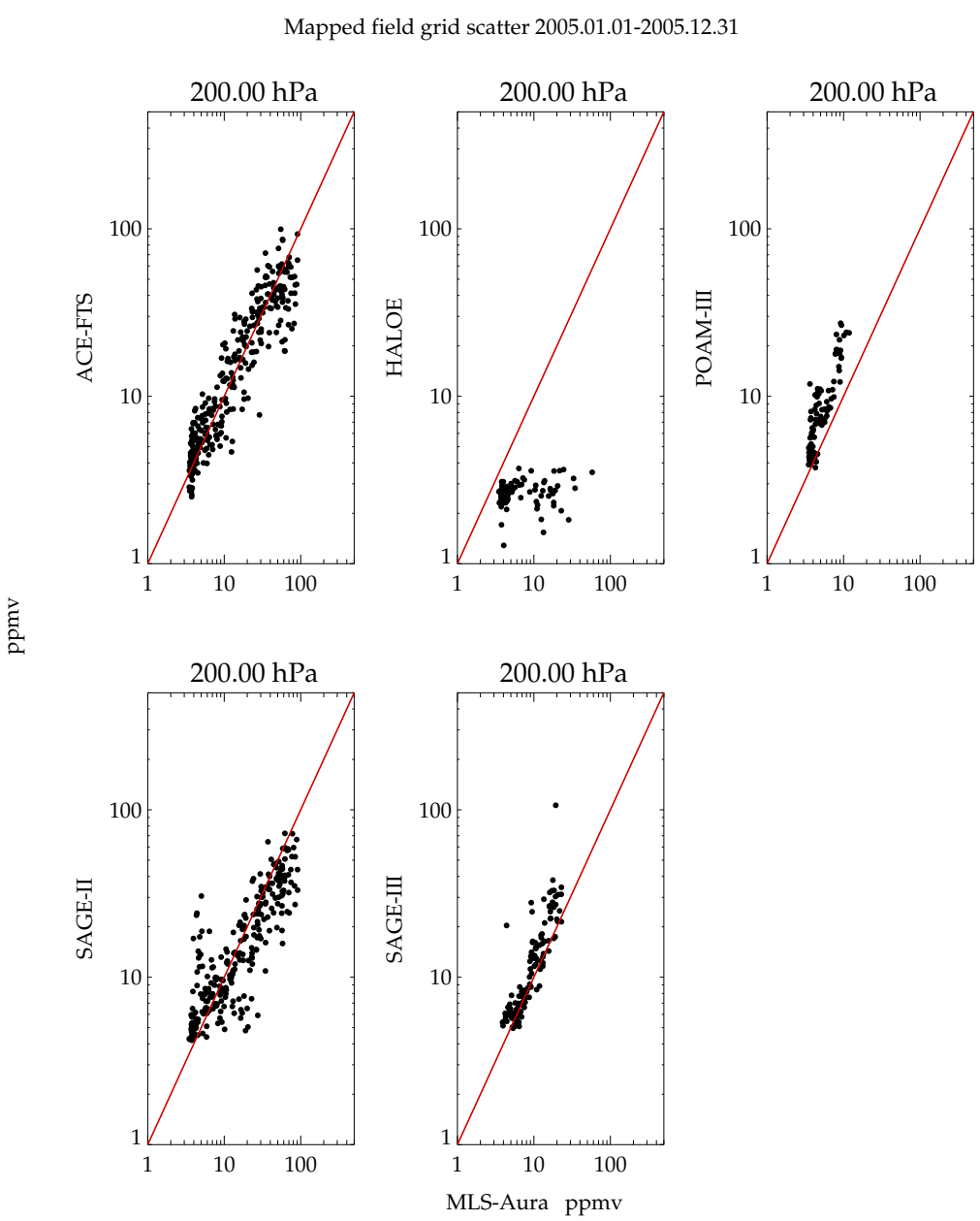

Figure S45. Scatter plot of mapped grid box values of humidity from occultation instruments versus MLS Aura at 200 hPa.

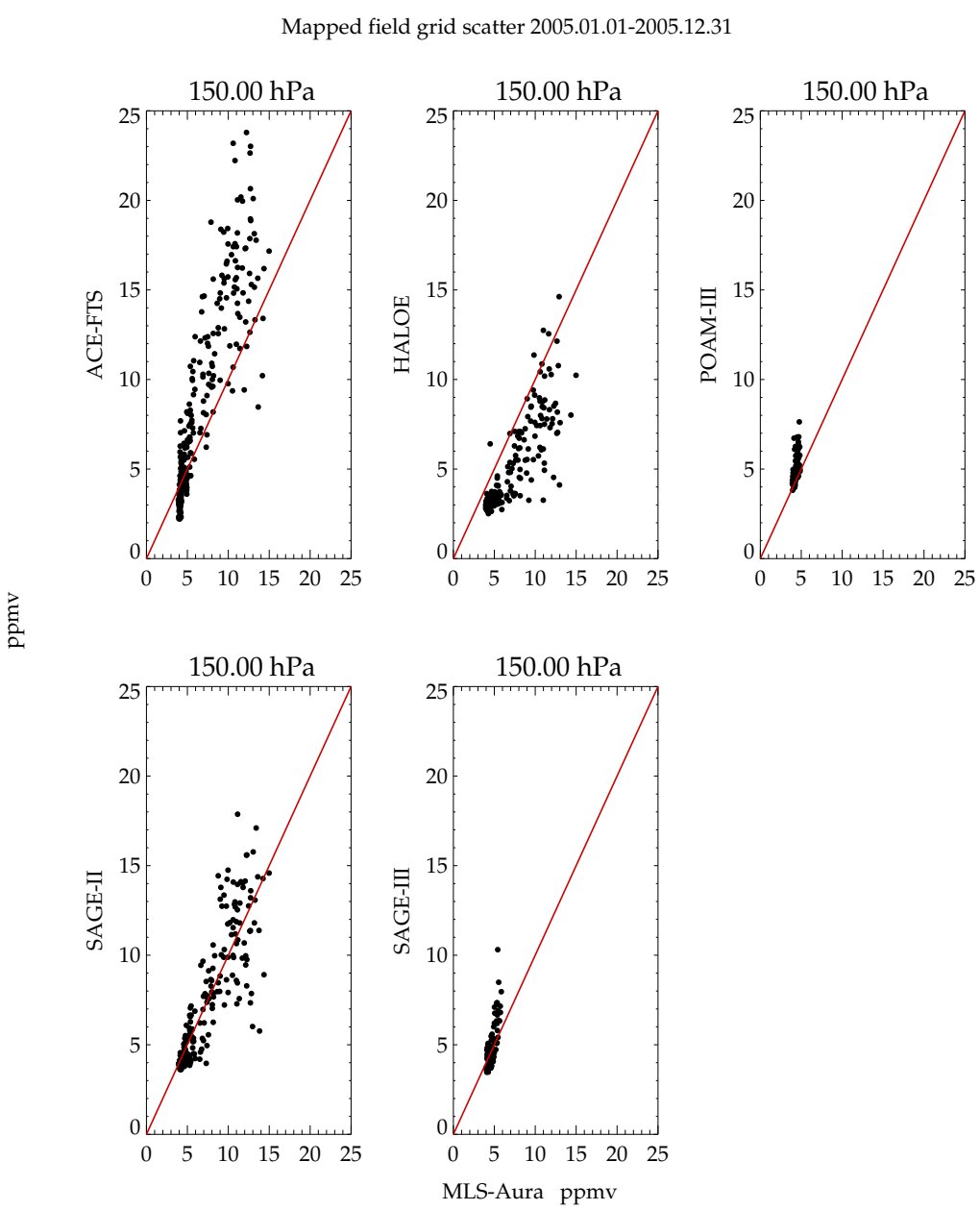

Figure S46. Scatter plot of mapped grid box values of humidity from occultation instruments versus MLS Aura at 150 hPa.